THE PENNSYLVANIA STATE UNIVERSITY

Phoenix Helicopter

Robert Aguece
Cristopher Henderson
Kevin Klohe
Dennis Larkin
Gregory Palencar
William Ripley
Dale Schulz

June 1, 2011

Proposal Summary

The Phoenix Helicopter is a multi-mission platform capable of performing a variety of missions including search and rescue, insertion, and resupply. This concept uses a rigid co-axial main rotor in combination with a pusher propeller to provide high speed capabilities. The propeller opens from 0 degrees of pitch to provide auxiliary propulsion to the helicopters at forward speeds beginning at 113 knots and higher. Normally, conventional helicopters use the main rotor to provide lift and forward flight power. Using the pusher propeller, The Phoenix can reduce the total power required by splitting the required power for forward flight to a more efficient auxiliary propeller at higher speeds. This power splitting results in less total power than conventional competitors and allows our configuration to reach speeds of up to 225 knots. The Phoenix also provides distinct advantages over tiltrotor systems as well. Tiltrotor systems are highly complex and although they have higher cruise altitudes and speeds the Phoenix provides the superior hovering capabilities of a conventional helicopter coupled with speed. A spacious interior allows for various layout configurations that meet any customer needs and is fully reconfigurable to allow for the various mission types. Reaching a gross weight of 16,415 lbs., the body is streamlined to reduce parasite drag with all components internalized, including engine, transmission, and retractable landing gear.

Phoenix Specifications

- Lifting capability of 4000 pounds plus crew
- Maximum Cruise Speed of 210 knots
- Mission Radius of 250 nm.
- 390 Gallon Capacity Fuel Tank
- Rotor Diameter of 45 ft.
- 2 Standard CT7-8A Engines
- Enhanced Avionics and Communication Systems
- Easily reconfigurable cabin for use in multiple missions
- Missile Warning and Counter Measures (Optional)
- IR Suppression Systems (Standard and Optional)
- Health Usage and Monitoring Systems (HUMS)

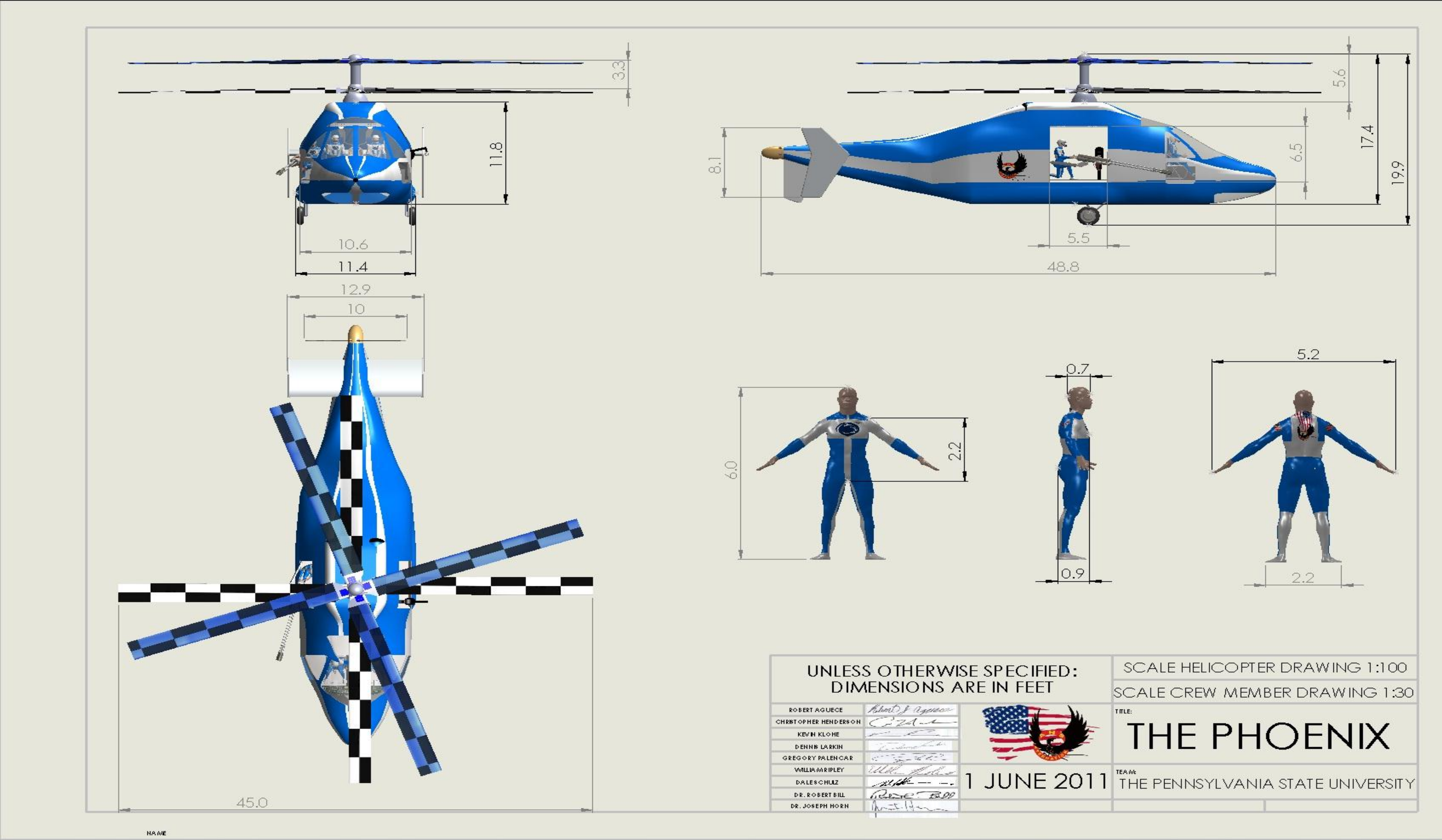

Figure 1. Three View Drawing of Phoenix with Dimensions.

Acknowledgements

We would like to extend our gratitude to the faculty; Dr. Robert Bill, Dr. Edward Smith, and Dr. Joseph Horn, that helped guide our helicopter design process and assist with any problematic areas that we came across. Also, our thanks go out to The Pennsylvania State University and more specifically the Aerospace Engineering Department for allowing this project to become part of our senior curriculum. Our personal mentor and Aerospace Department Secretary, Amy Custer helped to motivate us through this past school year and fully supported our work by showing strong enthusiasm. Our thanks go out to Zihiny Saribay, Mihir Mistry and Michael Pontecorvo for their assistance and support as well.

Signatures

The Pennsylvania State University Team

Robert Aguece	rja5028@gmail.com	Undergraduate Student
Christopher Henderson	cmh5291@psu.edu	Undergraduate Student
Kevin Klohe	klohe.kevin@gmail.com	Undergraduate Student
Dennis Larkin	djl5169@psu.edu	Undergraduate Student
Greg Palencar	grp5200@gmail.com	Undergraduate Student
William Ripley	wgr5004@gmail.com	Undergraduate Student
Dale Schulz	des5097@psu.edu	Undergraduate Student
Dr. Robert Bill	rcb28@psu.edu	Faculty Advisor
Dr. Joseph Horn	jfh19@psu.edu	Faculty Advisor
Dr. Zihini Saribay	zbs101@psu.edu	Faculty Advisor
Dr. Edward Smith	ecs5@psu.edu	Faculty Advisor

Posting Permission

We, The Pennsylvania State University and Senior AERSP 402 Design Team, hereby grant permission to the American Helicopter Society to allow this entry submission called The Phoenix to be posted on their website for the 28th Annual AHS Student Design Competition.

Dale Schulz (Team Captain)

Dr. Joseph Horn (Faculty Advisor)

Table of Contents

List of Figures

List of Tables

Down Select Process

Down selecting a single helicopter platform requires both quantitative and qualitative reasoning. Initially, helicopter platforms are introduced such as NOTAR, a ducted tilt rotor, a tilt rotor, two single main rotor compound variations, and a compound tandem. A qualitative study is done to take a closer look at known aircraft with the same features and determine if they can meet performance requirements and color values are input into an MS Excel spreadsheet. A few key proposal requirements driving the analysis are the high speed requirement for search and rescue and a large cargo area and capacity. Using the spreadsheet given in the Appendix with quantified colors the two highest values are selected and narrowed down to the Tilt Rotor concept and the Co-axial Compound concept.

Analysis is done to determine which of the two platforms will have better power performance and fuel burn capabilities. Several values needed to be set to keep the quantitative analysis similar. The assumed weight is set to 16,000 pounds, the forward speed set to 225 knots, and the pressure altitude to 6,000 feet at a temperature of 95 degrees Fahrenheit. The fuel consumption analysis follows each time step in the given flight procedure and uses the specific fuel consumption (SFC) of 0.452. With the speed requirement in mission one the fuel consumption for the co-axial compound uses 307 pounds less than the tilt rotor. The tilt rotor uses approximately 200 less horsepower to reach the speed requirement, however. Other factors that drive the decision are configurability, innovation, noise, and safety. The extra factors are analyzed qualitatively based on current configurations. Using these two numbers and the qualitative factors, the Co-axial Compound concept is chosen to be designed for the AHS competition.

Structures

The body of the Phoenix Helicopter is set to accommodate all mission requirements and is sized to fit cargo, crew, engines, transmission, fuel containers, electronics, retractable forward landing gear, and any other necessary equipment or functional parts. The cockpit windows allow for 180 degree visibility both horizontally and vertically. A sliding door is on either side of the aircraft to accommodate for the cargo to be tracked in either side on a permanent rail system, a detachable winch system, a gunner turret, or any add on feature requested. Both doors are 5.5 feet wide by 6.5 feet tall to allow for cargo crates that are 3 feet tall, 5 feet wide, and 7 feet long.

The overall dimensions of the structure, without rotor, propeller, and landing gear, is 11.81 feet tall, 46.67 feet long, and 10.61 feet wide above the sponsons. With the sponsons it reaches 11.45 feet wide as seen in Figure 1.

The empennage portion of the body has a 16 degree incline from the underbelly to allow for the propeller guard fin. The nose cone is 5.835 feet long. The cockpit is 8.33 feet long to allow for all controls, displays, seating, and other necessary equipment. The cargo bay is 18.5 feet long to allow for storage containers, gurneys, crew seating, and extra space for excess cargo boxes. The empennage structure is 14 feet long to house the frame support for the tail and propeller.

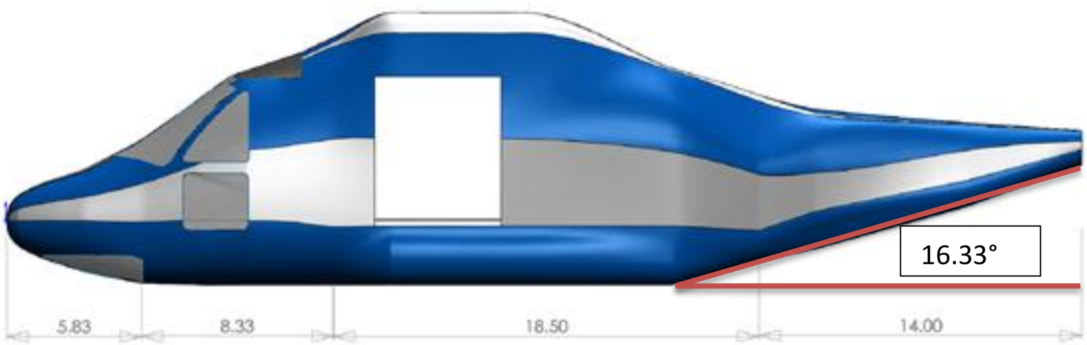

Figure 2. Side view of structure with dimensions

The roof on the body is built large enough to house two CT7-8A engines and a customized transmission along with the transmission support.

Empennage Size and Placement

The empennage size and placement is a unique challenge. The empennage is in the complex wake of the main rotor in some flight regimes while it may be outside the wake in other regimes. This makes the size and placement of the surfaces critical. The size of the vertical and horizontal stabilizer is determined through analysis of past co-axial platforms and plotting the disk area vs. size of the stabilizer. Figure 3 is the frontal view of the tail structure with both vertical and horizontal stabilizers present. One thing to notice is the center ring support. This piece of the structure acts as both the connection point for the tail to attach to the frame of the body and as a bearing support for the propeller shaft to minimize any bending of the shaft from input torque. No stress or strain analysis is done on this piece of structure because it is not attached to the frame and will not be accurately modeled.

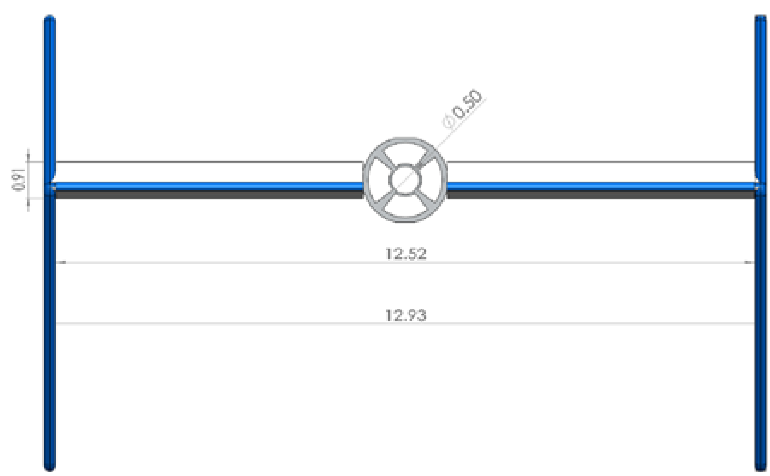

Figure 3. Tail Front View w/ Dimensions and Center Support Ring

The horizontal stabilizer area is based on a top down view of the surface. The total area is 40.66 square feet and a mark is placed on Figure 4 showing the relation between the Phoenix and other co-axial platforms. The area is calculated by taking the total length of the stabilizer, multiplying the 4.27 foot width by the 12.52 foot length and subtracting out 12.81 square feet for the portion of the stabilizer within the body. Figure 4 depicts the effective disk area of a single rotor. Our rotors both have a 22.5 foot radius. This puts the effective disk area at 1590 square feet. Our platforms horizontal area fits very well with the other platforms and qualifies as a suitable size.

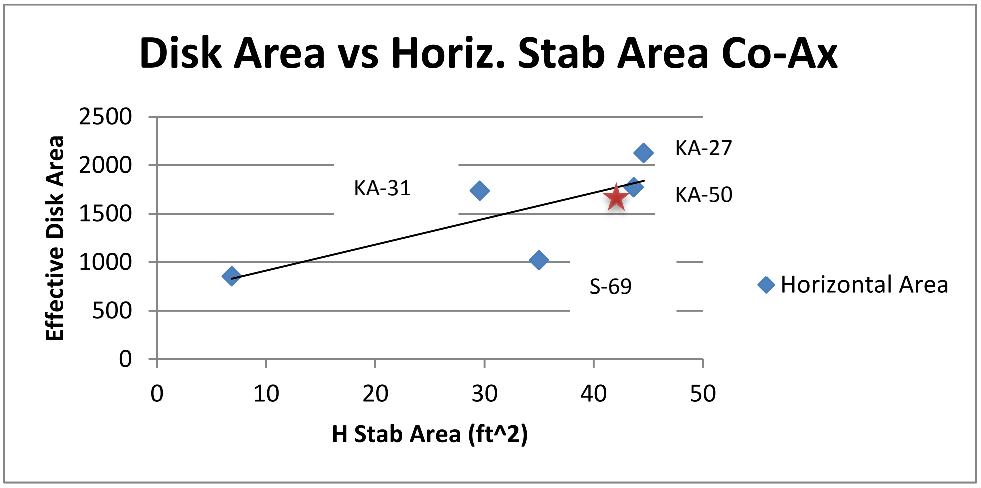

Figure 4. Disk Area v. Horizontal Stabilizer Area for Co-Axial Helicopter w/ Phoenix Mark

In Figure 5, the vertical stabilizer appears similar to the Sikorsky S-97 vertical stabilizer. The height is 8.12 feet and has a maximum width of 3.64 feet at the middle.

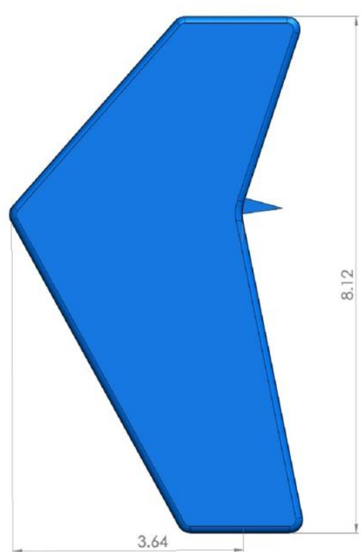

Figure 5. Vertical Stabilizer Plan Form w/ Dimensions

The vertical stabilizer area is based on having two vertical stabilizers, but the Phoenix has a propeller guard fin that also needs to be factored in. The total vertical surface area calculated is 58.26 square feet and a mark is placed on Figure 6, again showing the relation the Phoenix has with other co-axial platforms. The effective disk area is plotted versus the stabilizer area. Like the horizontal stabilizer, the Phoenix's vertical stabilizer is sufficient to work with our size rotor.

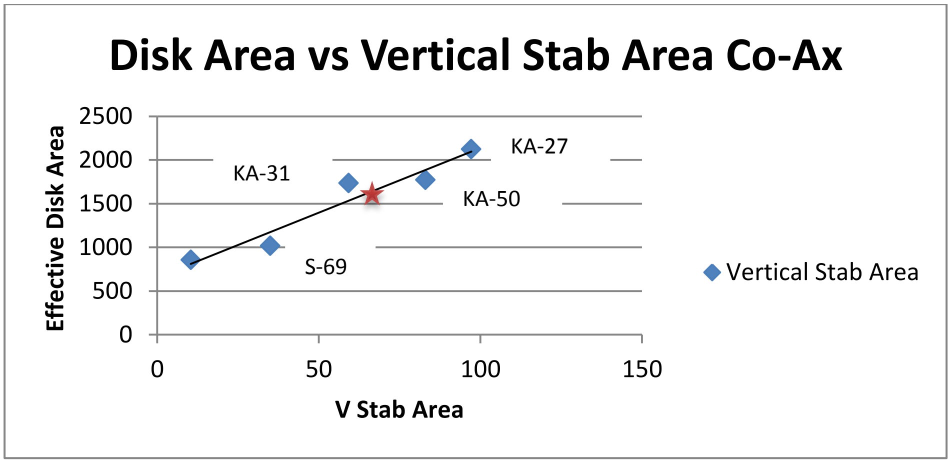

Figure 6. Disk Area v. Vertical Stabilizer Area for Co-Axial Helicopter w/ Phoenix Reference

The quarter chord of the horizontal stabilizer is placed 7 feet from the propeller which places it underneath the wake of the main rotors both in forward flight and hover. The propeller guard has a vertical edge that is 4.42 feet long and runs perpendicular to the propeller shaft to give the helicopter more safety features. The propeller has a 10 foot diameter and using the guard is necessary to keep the blades from reaching the ground on landing. As seen in Figure 7, the guard is an angled fairing that is used as another vertical stabilizer for the helicopter. Within the propeller guard is the rear landing gear.

Figure 7. Propeller Guard Side View

Reconfigurable Cabin

An important aspect of this design being a fully integrated aircraft, able to adapt to many various missions, is that it has a fully reconfigurable cabin. The three missions, as set forth by the AHS competition parameters, are Search and Rescue, Insertion and Resupply. All three missions require room for at least two pilots and auxiliary crew.

The Search and Rescue mission requires that the helicopter carry two empty litters, two medical personnel and up to 500 pounds of medical equipment during the outbound leg and either six passengers or two occupied litters, two medical personnel and up to 500 pounds of medical equipment. This requires there to be seats for up to six personnel that can be replaced with gurneys for rescued victims, yet still have enough room for the medical equipment. In order to do this, the gurneys have been utilized to double as bench seats. This enables the cabin to be easily changed for both the inbound and outbound configurations, and everything in between, see Figure 8.

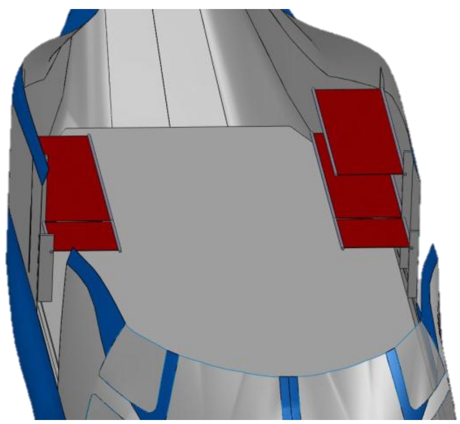

Figure 8. Reconfigurable Cabin for Search and Rescue

The Insertion mission involves carrying six troops and cargo up to a total of 4,000 pounds on the outbound mission and an empty cabin on the inbound. This mission is not difficult to accommodate, the six personnel have been allocated room with two gurneys as bench seats and the only thing left to adjust for is around 3,000 pounds of gear. This is done using military cargo containers rated for up to 5,000 pounds. These cargo containers, being seven feet long, five feet wide and three feet high, fit perfectly within the confines of the cabin, leaving enough room to be moved around as needed.

Originally, the cabin was designed entirely aft of the port and starboard loading doors, however, after many evaluations of the center of gravity location, it was found that this cabin configuration was not conducive to a more efficient CG, and thus, the cabin was revamped to accommodate this. The storage space for the cargo containers was moved forward of the loading doors, helping to bring the CG under the main rotor assembly, and closer to a desired location, Figure 9.

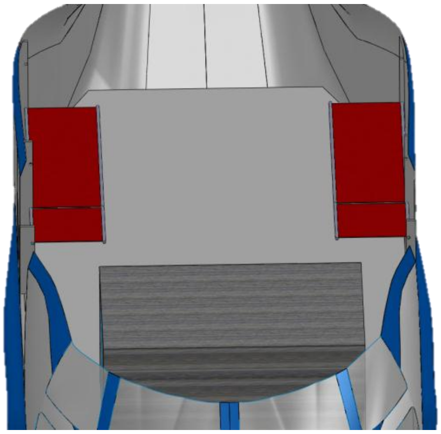

Figure 9. Cabin Arrangement w/ Forward CG Location

The final mission required for the AHS design competition is Resupply. This mission requires a payload of up to 3,000 pounds, both outbound and inbound, thus, the cabin was only organized to house up to two cargo containers without any excess passengers. The gurney seats are moveable and storable, giving more room within the cabin to move the cargo around, being much more flexible for CG relocation, as shown in Figure 10.

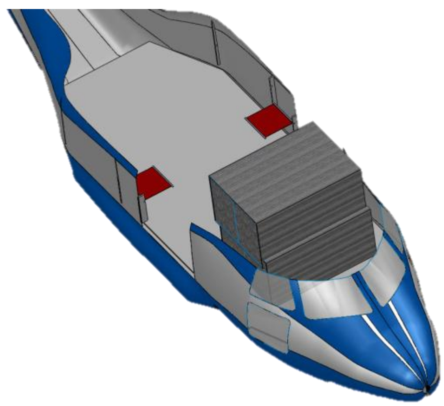

Figure 10. Insertion Configuration w/ Fully Forward CG Location

Transmission Support

The transmission mounts and engine support beams were modeled after the transmission mount design within the UH-60 Blackhawk main roof. The web dimensions are 6 inches long and .375 inches thick. The flanges are 6.125 inches long by .25 inches thick. Bringing the transmission within the body made the design simpler because it allowed for a non-curved beam that did not directly attach to the upper skin. Another benefit was allowing the engines to also attach to the beams within the body. As seen in Figure 11, the mount is designed to fit within the body of the helicopter. The length is 8 feet and width is 4.85 feet. These dimensions were chosen to keep within the limits of the body and still match similarly to the UH-60. The inner transmission support area measures 30 inches side-to-side and 29.75 inches front-to-back. These accurately measure to the UH-60 and apply dimensionally to the custom designed transmission as detailed later.

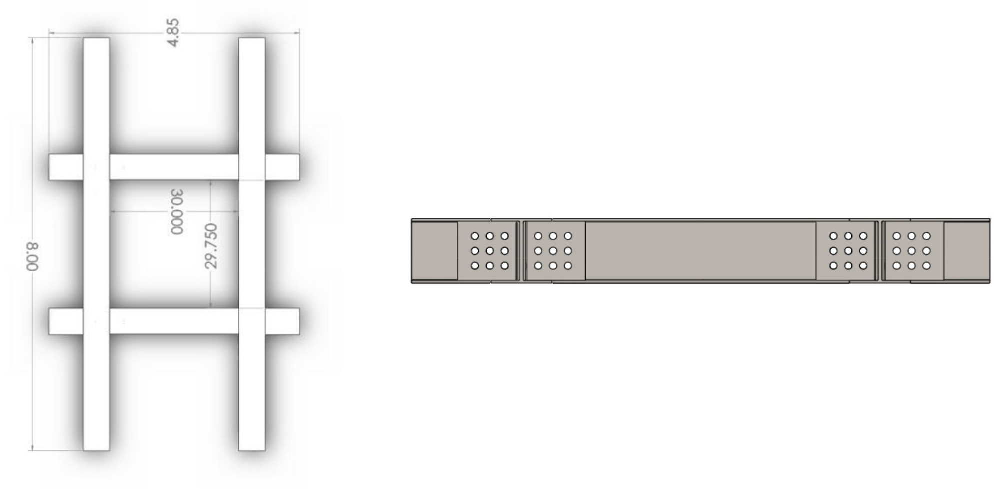

Figure 11. Transmission Support Top and Rear Views

There are 9 bolt holes per connection and each measure .75 inches in diameter. The structure is attached via .25 inch thick L-brackets that align with both I-beam webs. Each corner of the mated surfaces within the I-beam webs and L-brackets was chamfered to allow for a flush fitting. The material selected for the structure is 1095 (High Carbon) Steel with a modulus of elasticity of 30 million psi and a shear modulus of 11.6 million psi. The reason for choosing 1095 Steel is the higher properties over Titanium and Titanium alloys. The Tensile Strength of the Steel is 147,000 psi and is only 2 percent less than several Titanium alloys. Applying these properties into the SolidWorks Modeling Program and applying a distributed force to the main I-beams and the inner I-beams, the structure withheld a maximum required distributed force of 49,245 pounds to simulate a 3G load of the maximum predicted load of 16,415 pounds. The maximum predicted load is explained further under the Weight Analysis section.

The deflection under this 3G load is .472 millimeters, which occurs at the four inner corners surrounding the transmission. The maximum stress undergone within the structure is 28,991.9 psi and the maximum stress is 6.67726E-4 and both numbers occur at the outer corners of the I-beam flanges that are fixed. The ends of the beams were modeled as fixed supports and the bolts were modeled to withstand 100 N-m of torque. As modeled, the structure undergoes minimal stress at this load and all stress is localized to the main I-beam bolt holes and the adjacent L-bracket bolt holes.

Performance Analysis

The performance of the helicopter configuration was determined over a range of speeds using a blade element (BE) analysis and was programmed using MATLAB.

Important performance inputs concerning the design included gross helicopter weight (W), helicopter flat plate area (f), helicopter cg (center of gravity), rotor radius (R), rotor rotational velocity (Ω), rotor natural flapping frequency (ν_β), rotor spacing (S_r), rotor interference coefficient (κ), blade solidity (σ), blade twist (θ_{tw}), airfoil lift curve slope (a), airfoil drag divergence Mach number (M_{dd}), and auxiliary propulsor efficiency (η).

The analysis was executed using initial estimates for six stability/control angles and two thrust coefficients (C_{T1}, C_{T2}). The angles consisted of collective pitch (θ_o), differential collective pitch (θ_d), lateral cyclic pitch (θ_{1c}), longitudinal cyclic pitch (θ_{1s}), angle of attack (α), and bank angle (φ).

The six angles were iterated until the helicopter reached a near trim condition (condition where the force and moment equilibrium equations concerning the helicopter were approximately equal to zero) at respective velocity increments.

During the iteration the angles were used together with the performance inputs to calculate the rotor inflow, rotor flapping angles, and in turn the forces and moments acting on the helicopter so that a trim condition could be met for each respective velocity increment.

The rotor inflow (λ) was calculated according to momentum theory (uniform inflow) and was solved for numerically using a Newton-Raphson iterative approach. The equation for rotor inflow according to momentum theory is shown below.

$$\lambda = \mu\tan(\alpha) + \frac{C_T}{2\sqrt{\mu^2 + \lambda^2}} \qquad \text{Equation 1}$$

Because the rotor inflow during forward flight is not accurately described by momentum theory a Drees linear inflow model was used to adjust certain equations of the BE analysis. Equations for rotor coning angle (β_o), longitudinal flapping angle (β_{1c}), lateral flapping angle (β_{1s}), and thrust coefficient were adjusted according to the Drees model.

The Drees model consists of longitudinal and lateral inflow gradients (k_x, k_y). The equations for the inflow gradients are listed below. Notably, the longitudinal inflow gradient is dependent upon the wake skew angle (χ) and the advance ratios defined parallel and perpendicular to the rotor disk (μ_x, μ_z).

$$k_x = \frac{4}{3}\left(\frac{1-\cos(\chi) - 1.8\mu^2}{\sin(\chi)}\right) \qquad \text{Equation 2}$$

$$k_y = -2\mu \qquad \text{Equation 3}$$

$$\chi = tan^{-1}\left(\frac{\mu_x}{\mu_z + \lambda_i}\right) \qquad \text{Equation 4}$$

The helicopter forces and moments calculated during the BE analysis consisted of rotor thrust (T), rotor torque (Q), rotor side force (Y), rotor drag (H), rotor rolling moment (M_x), rotor pitching moment (M_y), fuselage drag (D_f), and fuselage download (L_f). Effects of a horizontal stabilizer were included in the force and moment equilibrium equations.

The auxiliary thrust (T_{aux}) for the helicopter configuration was determined assuming that the auxiliary propulsor would counteract a certain percentage of the helicopter flat plate area (this certain percentage was denoted as f_{aux}). The power required to drive the auxiliary propulsor was dependent on the auxiliary thrust value. Equations for auxiliary thrust and auxiliary power are shown below.

$$T_{aux} = \frac{1}{2}\rho V^2 f_{aux} \quad \text{Equation 5}$$

$$P_{aux} = \frac{T_{aux}V}{\eta} \quad \text{Equation 6}$$

The power required to drive the main rotor was calculated from the rotor torque determined from the BE analysis. The equation for rotor power is listed below.

$$P_{rotor} = Q\Omega \quad \text{Equation 7}$$

Rotor Rotational Velocity Reduction

The hover tip speed (ΩR) for the helicopter configuration was chosen to be 680 ft/s. Values for ΩR of conventional helicopter platforms range from 680 – 730 ft/s. An ΩR value of 680 ft/s was chosen for the design to help reduce helicopter noise. The rotor radius (R) was chosen to be 22.5 ft which yielded a rotor rotational velocity (Ω) value of 30.2 rad/s (288.6 rpm).

It was decided that Ω would be significantly reduced during forward flight to help promote higher forward flight speeds. A low Ω value allows for high forward flight velocities because the onset of drag divergence (dramatic increase in power due to increased drag) is delayed.

The approach towards the Ω reduction was as follows – when the advancing tip Mach number ($M_{tip,adv}$) reaches the drag divergence Mach number (M_{dd}) lower Ω so that the advancing tip speed ($V_{tip,adv}$) is equal to the hover tip speed. Two values had to be determined, the reduced Ω value and the velocity at which the reduction would take place (V_∞). At the reduction velocity the auxiliary propulsion would be engaged.

An M_{dd} value of 0.78 and a design point temperature of 59 ^{o}F (15 ^{o}C) was chosen. The reduced Ω value and the reduction velocity were determined using the equation shown below, where $\boldsymbol{a}$ is the speed of sound.

$$V_{tip,adv} = \Omega R + V_\infty = M_{tip,adv}a \quad \text{Equation 8}$$

An ΩR value of 680 ft/s, an $M_{tip,adv}$ value of 0.78 (equal to the M_{dd} value), and an a value of 1117 ft/s (speed of sound at 59 ^{o}F) yielded a reduction velocity of 113.3 kts (191.2 ft/s).

Setting $V_{tip,adv}$ equal to 680 ft/s and using R and V_∞ values of 22.5 ft and 113.3 kts yielded a reduced Ω value of 21.7 rad/s (207.5 rpm). The original Ω value would be reduced 28.1%.

(Note: Due to restriction on gear sizing, Ω was reduced to 21.8 rad/s (208.4 rpm) – 27.8% reduction)

Temperature affects the speed at which the Ω reduction takes place because the advancing tip Mach number depends on the speed of sound which depends on temperature. A reduced temperature gives a lower value for speed of sound which gives a higher value for advancing tip Mach number (for a given advancing tip speed). This means that the advancing tip Mach number reaches the drag divergence Mach number at a lower forward flight velocity.

A design point temperature representative of sea level was chosen as opposed to a temperature of 95 ^{o}F so that premature drag divergence (drag divergence before the Ω reduction) would not occur at a sea level flight condition. If a design point temperature of 95 ^{o}F was chosen premature drag divergence would occur at a sea level flight condition.

Helicopter Power

The performance of the helicopter configuration was determined up to a speed of 250 kts. The power vs. speed curves for two flight conditions, 6K95 (ρ = 0.001781 sl/ft^3) and sea level (ρ = 0.002378 sl/ft^3), are shown in Figure 12 and Figure 13.

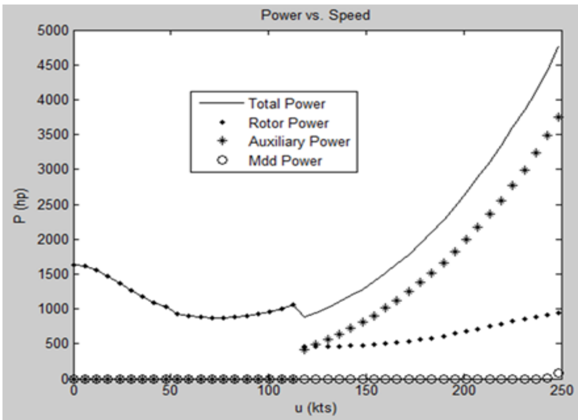

Figure 12. Power vs. Speed, 6K95 (ρ = 0.001781 sl/ft3)

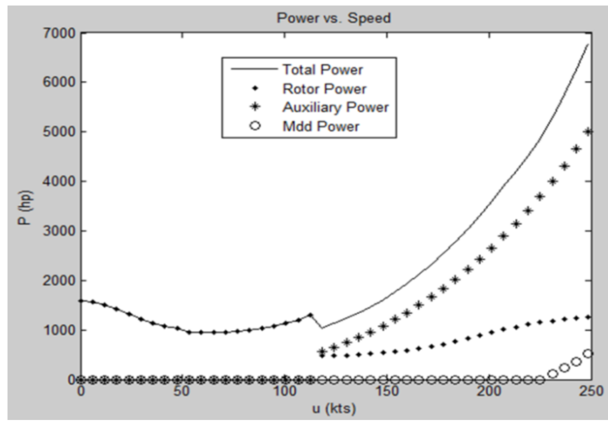

Figure 13. Power vs. Speed, sea level (ρ = 0.002378 sl/ft3)

It can be seen in the figures that at a speed of 113.3 kts the rotor rotational velocity (Ω) is reduced and the auxiliary propulsion is engaged. In the two flight conditions shown above the auxiliary propulsor is assumed to counteract 100% of the helicopter flat plate area (f). Thus it is assumed that the auxiliary propulsion produces a substantial portion of the propulsive thrust required to drive the helicopter once the Ω reduction velocity is reached. This results in a majority of the installed helicopter power going towards driving the auxiliary propulsor instead of the main rotor.

The power increase due to the onset of increased drag (drag divergence), notably in **Error! Reference source not found.**, was calculated according to the equations listed below.

$$if\ M_{tip,adv} > M_{dd} \qquad \text{Equation 9}$$

$$\Delta M_{dd} = M_{tip,adv} - M_{dd} \qquad \text{Equation 10}$$

$$C_{p,M_{dd}} = 0.007\Delta M_{dd} + 0.052\Delta M_{dd}^2 \qquad \text{Equation 11}$$

$$P_{M_{dd}} = 2C_{p,M_{dd}}\rho A(\Omega R)^3 \qquad \text{Equation 12}$$

The performance inputs, thrust values, and power values for Figure 12 and for Figure 13 can be found in the appendix.

Main Rotor

Figure 14. Overall Main Rotor

The main rotor was defined by the following performance attributes, Table1:

Rotor Radius	22.5 ft
Solidity	0.12
Blade Twist	-10 degrees
vβ	1.6
Omega 2	208.4 rpm
Max Available Power	5200 hp

Table 1. Main Rotor Design Parameters

Main Rotor Shafts

This main rotor will be explained from the inside and worked outward. This starts with the sizing of the main rotor shafts. They were sized by using shear stress analysis for the two separate shafts. The first equation used was one that took power (HP) and rotational speed (rpm) to convert into a torque (lbf.*ft.), Equation 13. The value of 33000 (lbs.*ft./min) is a conversion constant and 2π converts (rpm) into (rad/min). The next equation used was a basic shear stress equation for a cylinder which took the torque found in Equation 13 and shear strength for a given material to find the inner and outer diameter of the shaft, Equation 14. The value of 12 is used to convert from feet to inches and 16/ π is from the polar moment of inertia.

$$P = \frac{Torque * 2\pi * \text{rotational speed}}{33000} \quad \text{Equation 13}$$

$$\tau_{max} = \frac{Torque * 12 * 16 * OD}{\pi * (OD^4 - ID^4)} \quad \text{Equation 14}$$

$$\sigma_{yield} = \frac{Force}{\pi\left[\left(\frac{OD}{2}\right)^2 - \left(\frac{ID}{2}\right)^2\right]} \quad \text{Equation 15}$$

The power used to size each rotor was found by putting a 1.5 factor of safety on the Max Available Power to account for maneuvering, 7800 HP, and using a 2/3 power split between the rotors to account for differential yaw, 5200 hp. This case would simulate one rotor shaft taking all the power in one 30 second burst because the Max Continuous Power is only 2200 hp. and Max Available Power is 5200 hp. The rotational speed used, 208.4 rpm, is only during forward flight above 113kts when the prop is engaged and is the lowest rotational speed. The max shear strength was chosen by using the material Titanium Ti-5AI-25Sn with the following properties, Table2:

Shear Strength	75.4 ksi
Yield Tensile Strength	120 ksi
Density	0.162 lb/in^3

Table 2. Material Titanium Ti-5AI-25Sn Properties

Using the shear strength given, the following dimensions were found for the shafts, Table3:

	Inner Shaft	Outer Shaft
Inner Diameter	5"	6.5"
Outer Diameter	6"	7.25"

Table 3. Shaft Inner and Outer Diameters

In order to reach the tensile strength limit given in Table2 and using Equation 15, the shafts would have to undergo a tensile force of over 1,000,000 lbs. After the shafts, the swash plates need to be designed.

Swash Plate Design

This was by far the most complicated design in the main rotor assembly. The swash plate controls the pitch angles of the blades and must be able to rotate freely about a point in order to individually control each blade. Finding the exploded views of the QH-50 was a tremendous help in the design process because it is very difficult to decipher each individual link in other main rotor assembly pictures that were found, Figure 15, Figure 16 and Figure 17. These pictures helped design the collective, lateral, and longitudinal pitch inputs of the blades. The differential collective was created in house because there were no detailed schematics of this essential attribute needed to control yaw for a co-axial helicopter.

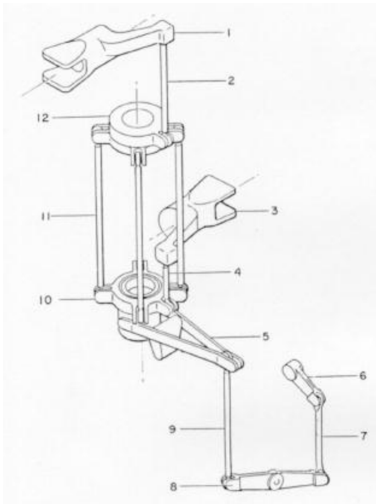

Figure 15. QH-50 Collective

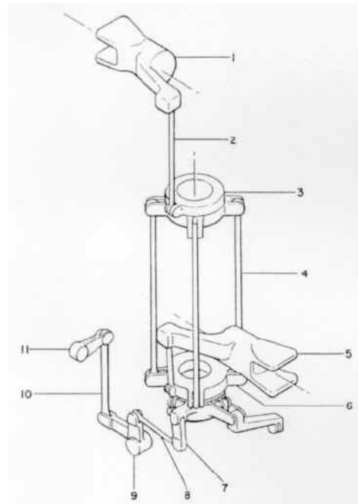

Figure 16. QH-50 Lateral

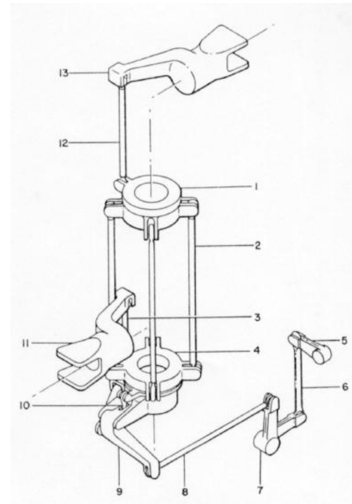

Figure 17. QH-50 Longitudinal

****The only time the differential collective changes its separation distance from the swash plate below it is when yaw control inputs by the pedals are triggered by the pilot. Please keep this in mind while looking at* Figure 18*. The parts in red are the differential collective and translate the motion of the other control inputs. Only the lower rotor was included in* Figure 18 *for zoomed in visuals of control inputs and swash plate control.* ***

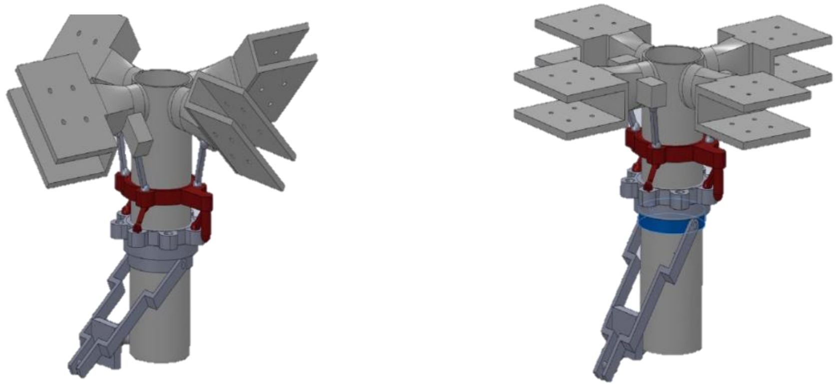

Figure 18. Collective Pitch Comparison

Figure 18 depicts the collective pitch comparison between the QH-50 and modeled design. As stated before, the differential collective, red parts, stays the same distance away from the swash plate below it. This changes the pitch on the blades equally and in the same direction. These pictures show how pitch changes as the collective is toggled.

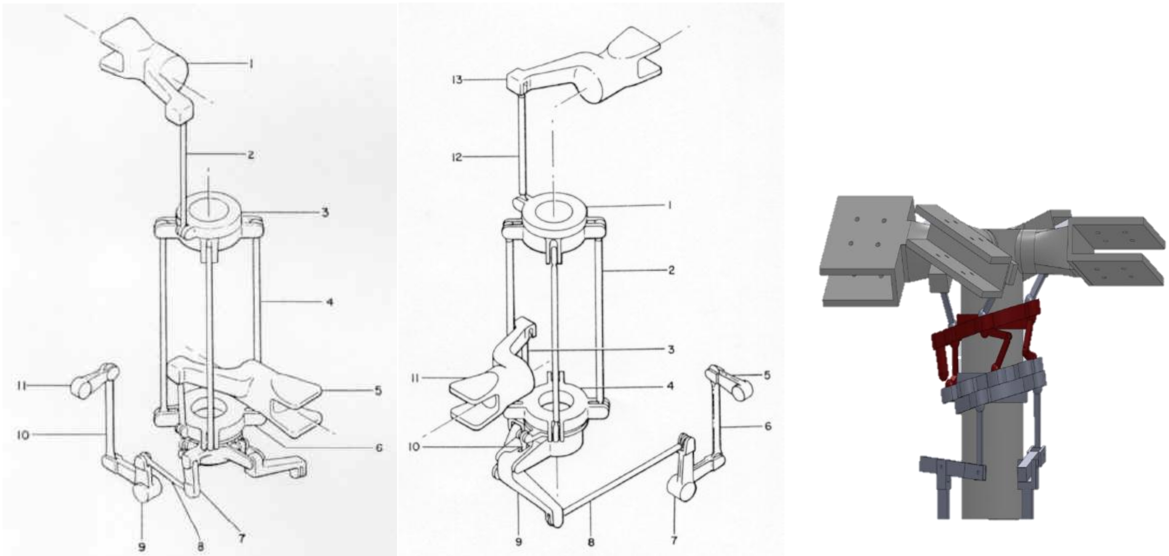

Figure 19. Lateral and Longitudinal Pitch Comparison

Figure 19 depicts the lateral and longitudinal pitch comparison between the QH-50 and modeled design. As stated before, the differential collective, red parts, stays the same distance away from the swash plate below it. The picture of the modeled design clearly shows independent pitch control for pitch and roll scenarios. The lateral and longitudinal control input moment arms are at different angles, one slightly angled down and the other angled up. The swash plates are clearly tilted in a parallel manner in order to translate the inputs and the blade clamps on either side have different pitch, the left having more pitch than the right.

There were no sources found to properly depict differential collectives. A differential collective, in the way it was modeled, changes the collective pitch on the lower rotor. This was done by having an outer ring surrounding the swash plates and used similarly to the regular collective, Figure 20. The regular collective stays in the same position, leaving the upper rotor at a constant pitch. This is done while the differential collective shifts to change the pitch on the lower rotor, thus controlling yaw inputs from the pedals. The figure below shows the differential collective shifted slightly upward to change pitch.

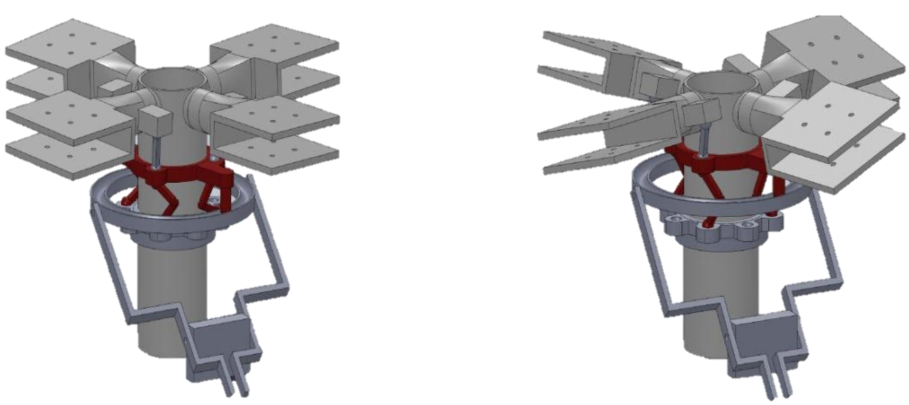

Figure 20. Differential Collective

Rotor Separation

After the control inputs were finished, the rotors had to be. The rotor separation was agreed upon the value of 40” because it was based off the XH-59 platform. The variable we based this off of was blade rigidity, vβ. The XH-59 had a rotor diameter of 36’ and a rotor separation of 30”. Since our aircraft had a similar rigidity, 1.6, we scaled out rotor separation to fit our larger rotor diameter. The main rotor has a diameter of 45’ and a separation of 40”. There is 18” between the lower rotor and the ceiling of the fuselage to leave room for the control inputs, Figure 21.

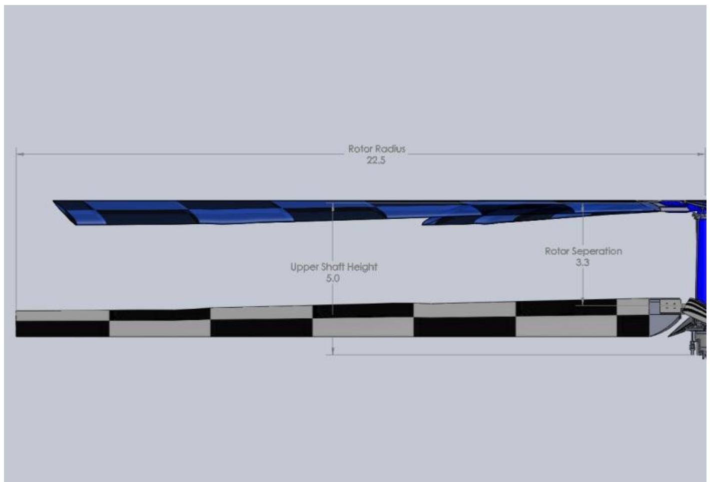

Figure 21. Rotor Separation

Fairings

The fairings were put around the inputs and links in order to decrease the drag on the hub, especially in forward flight. The fairings saved around 400 HP at 200 kts. in the 6K95 condition. Even though bulkier, the fairings take away the dynamics of the spinning pitch links through the air allowing for smoother flight, Figure 22. The fairings from the presentation were made larger in order to allow full range of blade clamps.

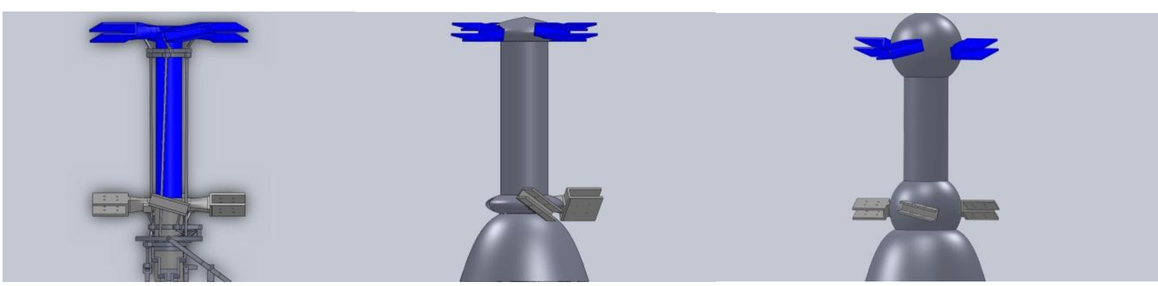

Figure 22. Fairing Progression

Rotor Blades

The airfoils for the rotor blades were selected with a few key elements in mind: a high lift producing profile was necessary for hover and an airfoil with a high Mach divergence drag number was required for the high rpm applications. Three high lift airfoils and Three high speed airfoils were selected for evaluation under the operational parameters of the blades; the Boeing Vertol VR-12, Onera OA209, NASA RC(4)-10, Boeing Vertol VR-15, Onera OA206 and NASA RC(5)-10, respectively.

The airfoils were tested using XFOIL analysis software. For the sake of analysis, the high lift portion of the blade was assumed to be the innermost 80% while the high speed portion of the blade took up the remaining 20%. Using the assigned rpm values and other operating variables, the Reynold's Numbers were used in a sweep along the blade radius, providing an accurate depiction of the lift profile created along the blade length. The lowest red line in Figure 23 corresponds to the inner most portion of the blade. As the lines increase along the C_l/C_d curve, the portion of the blade each line corresponds to a further progressing outward portion of the blade from the hub. This increase is an incremental increase in velocity.

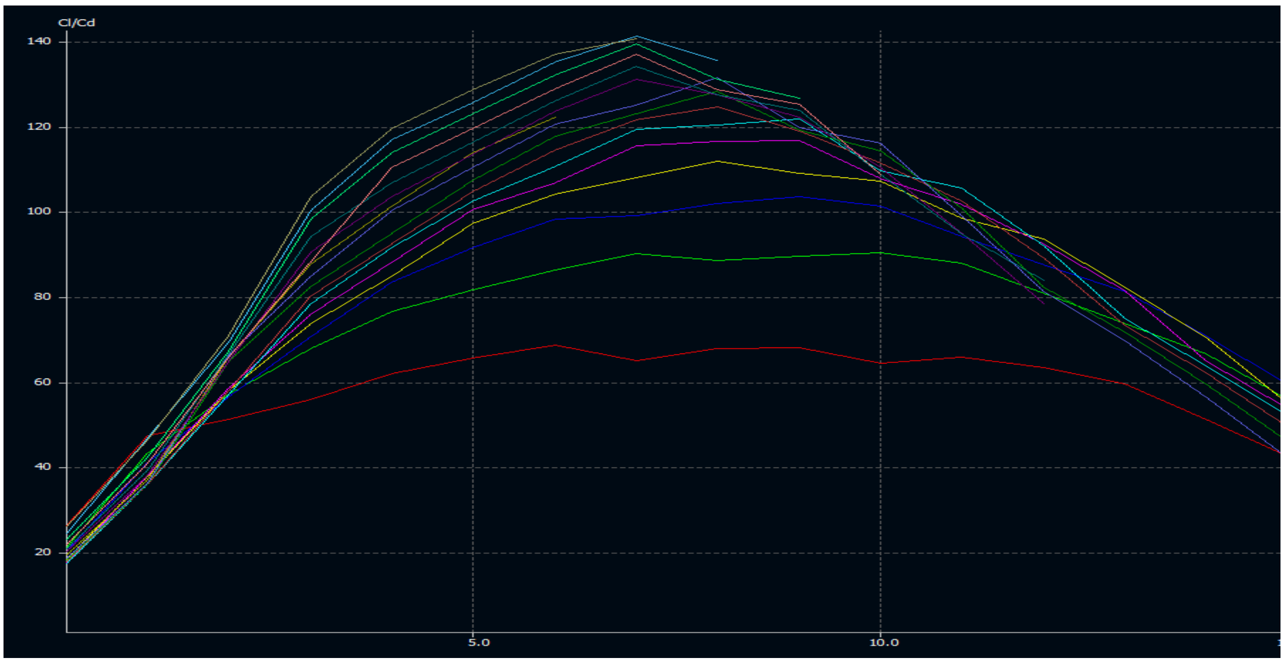

Figure 23. L/D v. α At Various Reynold's Numbers – Boeing Vertol VR-12

When running the high lift airfoils, the most important consideration was simply for a high L/D_{max}. Of the three high lift airfoils, the Boeing Vertol VR-12 had not only the highest L/D_{max} but also a more uniform lift profile when compared to either the Onera OA209 or the NASA RC(4)-10, as depicted in Figure 23.

The process was a bit different for the high speed airfoils. A Reynold's Number sweep was again used in the analysis, however, the values were done at increasing Mach numbers, in order to find the M_{dd}, the point at which the airfoil begins to fail and is no longer able to produce any lifting forces. The Boeing Vertol VR-15 performed the best, with an approximate M_{dd} of 0.91, where the failure of the airfoil is illustrated in Figure 24. The Onera OA206 and NASA RC(5)-10 had respective M_{dd} values of 0.87 and 0.67.

Once the airfoils were chosen for the blade, the physical dimensions needed to be identified. Using the solidity and rotor radius, defined previously in Table 1, the blade chord was found to be 2.21 feet. The blade twist was defined in order to produce a constant lift profile along its' entire length.

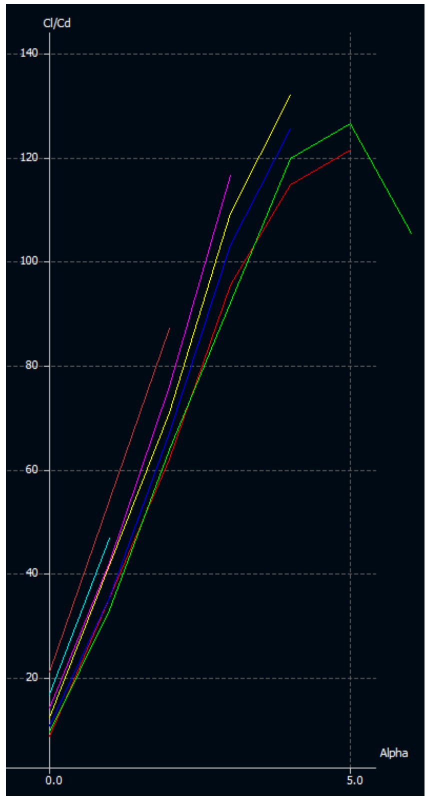

Figure 24. L/D v. α Airfoil Failure At A Mach Number of 0.91 – Boeing Vertol VR-15

As stated before, the colored lines beginning with red and moving up and to the left, correspond to progressing outward distance increments of separation from the hub. The increments are increasing velocity points.

Auto Rotation

One key advantage that Phoenix possesses over tilt-rotor platforms is the ability to auto rotate. An auto rotation analysis was done by comparing the Phoenix's autorotation index to that of other platforms with acceptable auto rotation performance. The autorotation index is a way of measuring the stored energy in the main rotor. An autorotation index based off of those used by Sikorsky, which is weighted by the disk loading was used and also used to build the figure below (Leishman, 2006).

$$AI = \frac{I_R \Omega^2}{2W * DL}\ (Leishman\ Eq. 5.93) \qquad \textbf{Equation 16}$$

Where I_R is the inertia of the main rotor, 4196 slug*ft^2, Ω is the rotational speed of the rotor in low speed flight conditions, 30.2 rad/s, W is the estimated weight of the rotorcraft 16000 lbs, and the DL, Disk Loading, is thrust divided by disk area, 10.06 lbs/ft^2. With these values the auto rotational index is 11.88. This AI with a disk loading of about 10 the Phoenix is comparable to the auto rotational characteristics of the UH-60 Blackhawk.

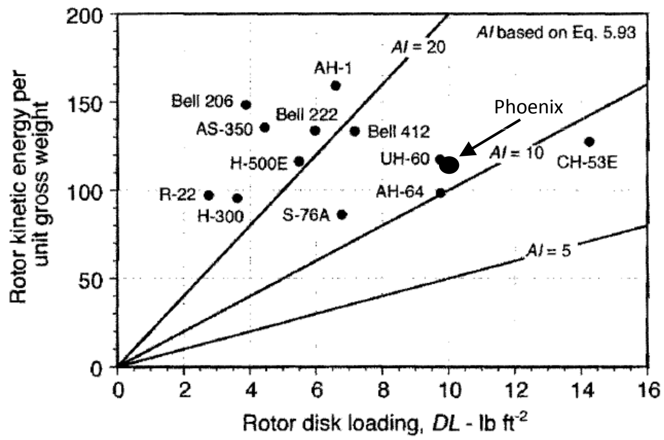

Figure 5.29 Autorotative indices derived for several helicopters at standard sea level conditions. Data source: Various published helicopter specifications.

Figure 25. Auto Rotation Index of Various Helicopters and the Phoenix

Transmission and Drive Train

The high-speed flight regime that the helicopter is aiming to work in required the design team to overcome the problem of drag divergence at the tips of the advancing blades. The solution chosen to defeat this problem was to use a multi-speed transmission to adjust the rotors rotational rate. The rotor will have two fixed speeds, high speed and low speed. While operating at low forward flight speeds the transmission will be shifted to the high-speed gear set and during operation at high forward flight speeds the transmission will be shifted to the low speed gear set. The shifting scheme will slow the rotational rate of the rotor at high forward flight speeds to reduce the apparent flow velocity over the blade tips avoiding reaching drag divergence. The forward flight velocity where the shift will occur was determined to be 113 knots based on the aerodynamic properties of the rotor. The design of the shifting gearbox was based on making the advancing blade tip velocity decrease at that speed to the tip speed at hover, which is 680 ft/s. In hover condition the desired rotational rate of the rotor is 288.59 rpm, which is the transmission's high-speed. After shifting at 113 knots forward flight speed in order to obtain the advancing tip velocity of 680 ft/s again the rotational rate of the rotor decreases to 208.7 rpm, transmissions low-speed. The previously presented rotational rates deviated slightly from these values originally but were finalized to these values due to the available reduction ratios.

The drive-train is powered by two CT7-8A turbine engines that are produced by General Electric. The standard dimension of the engine is a 26 inch maximum diameter and 48.8 inch length. The engine also comes in at a dry weight of 542 pounds. The specific fuel consumption at takeoff is 0.452 and has 2,634 shaft horsepower takeoff rating and both are found at sea level. The CT7-8A also provides Full Authority Digital Electrical Control (FADEC), which allows for easier manageability for the pilot. The engines drive the system with an input speed of 21,000 rpm. This input speed value was found from the certification test sheet provided in the appendix.

Knowing the initial and final drive speeds the total reduction ratios have been found to be 72.76:1 for the transmission in high-speed and 100.62:1 for low speed. The difference in reductions will be made by a two speed compound planetary transmission. All reductions through gearboxes except the compound planetary will be constant whether the transmission is in high-speed or low-speed.

Considering the fact that there are two power plants in the drive-train their outputs need to be combined to feed the power required to the rotors. Also the rotor output shafts are in line with the length of the fuselage. With both of these considerations in mind it was decided to run the engines output shaft into a spiral bevel gear box that turns the orientation of the shaft towards a combiner box. This 'turn box' will be integrated into the main transmission casing and be connected physically to combiner box

The combiner box has a total of four shafts coming into it and is integrated into the main transmission box. Two of the four shafts will be driving and come from the turn boxes and two will be driven.

The two driving pinions will be connected to a driven gear, which will be the power combining gear. The combining gear shaft feeds directly into the planetary gear set and is attached to the sun gear. The second driven gear is also meshed with the combining gear and transmits power to the pusher prop.

At this point it was decided to reduce the engine rpm going into the planetary gear set in order to avoid extremely high rotational rates of the spur gears which would require extra analysis to avoid their failure due to their own inertial force pulling them apart, their mesh rates and tooth loading. In order to determine these pre-planetary reductions it was necessary to look at possible reductions ratios within in the planetary gear set. In order to keep the size of the planetary gear set within realistic physical boundaries of the vehicle, and physical possible combinations for the gear box it seemed that the planetary gear set in the way that we intended to use it would not produce a reduction greater than 6:1. With this knowledge and the understanding that the bull gear needed to be able to fit on the vehicle it was decided to make the bull gear reduction 5:1 and the turn-box as well as the combiner gear, in relation to the driving gears, 2:1 reductions. This gave a total reduction so far of 20:1 leaving the planetary to bring the drive-train to the desired final reduction ratio. With the previously stated values the required planetary gear reductions were able to be calculated and determined to be 3.63:1 in the transmissions high-speed set and 5.03:1 at the low speed set. As previously stated above the values used are the final design values. Initial guesses were made and then refined based on physically possible combinations for the planetary set.

From analysis of the prop it was found that the pusher prop would need a rotational speed of 3500 rpm to operate at the desired performance. In the beginning of the design phase the pusher prop was going to be driven after the planetary reduction. However, after determining that it needed to operate at such a high rpm it was decided to drive it off of the combiner gear, which rotates at 5250 rpm, and has a reduction ratio of 1.5:1. The pusher prop drive shaft will have a dual clutch in its direct driveline to allow it to be stopped for safety reasons on the ground as well as low speed flight. The clutch will be a wet disc pack clutch in order to reduce size. The dual action clutch will break the aft shaft and be disengaged with the driveshaft or engaged with the driveshaft and the breaking set disengaged. The clutch will also be integrated into the main transmission casing.

Gear Sizing

The gear sizing was determined for the spiral bevel gears using AGMA standard 431.01 (Committee, 1974) with the basis of using case-hardened steel. Displayed below is a basic flow chart of the power from the engine into the planetary gear set.

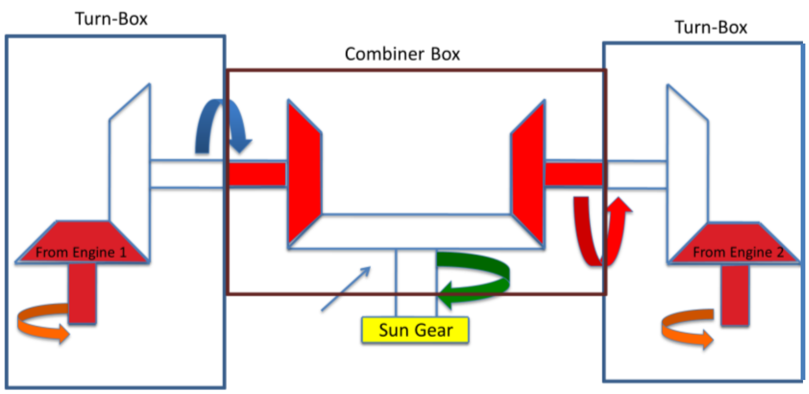

Figure 26. Flow Chart of Power Transfer from Engine

The turn-box and the combiner comprise all of the spiral bevels gears totaling 7 gears. The turn boxes are mounted to either side of the main transmission. The combiner box is integrated into the main transmission casing.

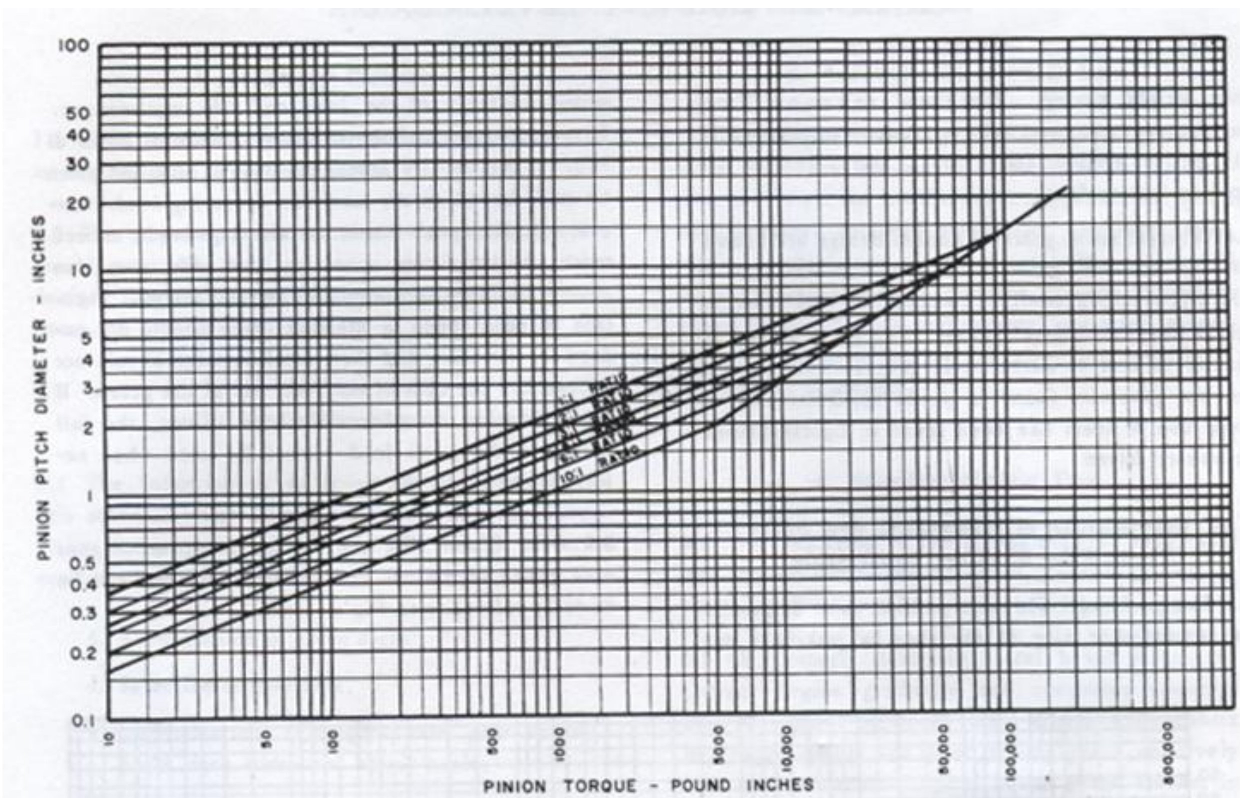

Figure 27. Pinion Pitch Diameter vs. Pinion Torque

The pinion pitch diameter for the spiral bevel gears was found using the above A.G.M.A. Standards graph. The torque loads were found for each input pinion and then correlated to a pitch diameter based on the appropriate reduction ratio. The gear driven by the pinion was sized according the ratio required since the pinion is the critical member and the driven gear will have no problem bearing the loads placed on it by the pinion.

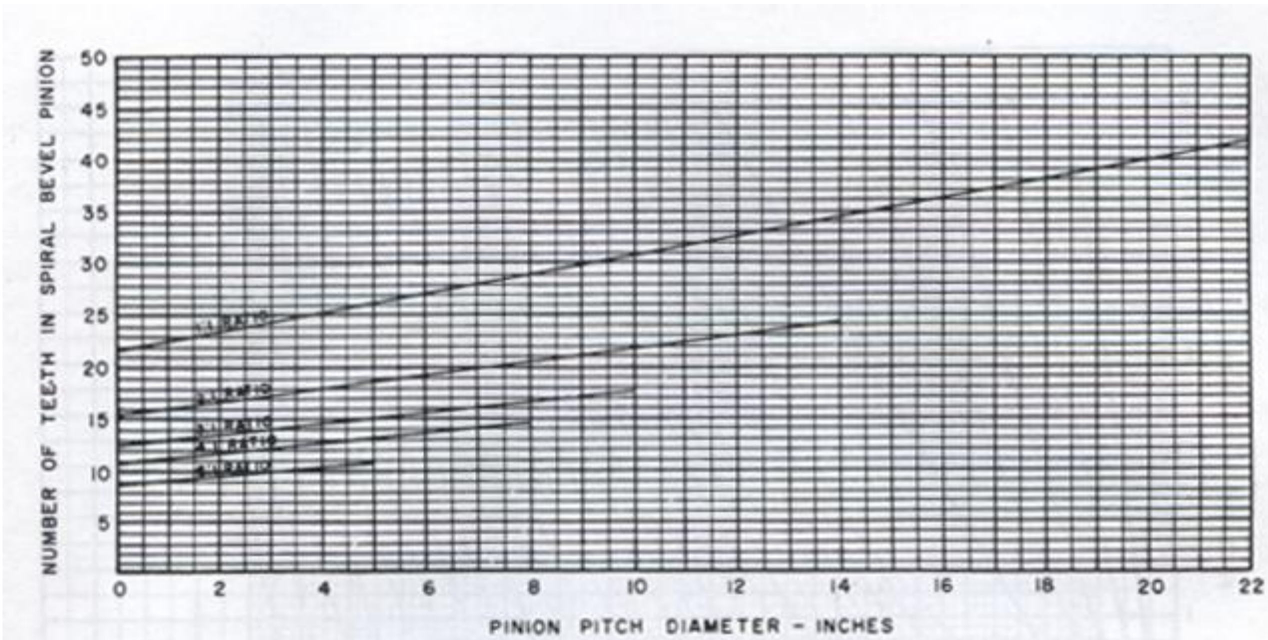

Figure 28. Number of teeth in Spiral Bevel Gear Based on Pinion Pitch Diameter

Using the pinion pitch diameter found earlier the appropriate amount of teeth was found using the above graph with the corresponding reduction ratio. The driven gear was once again just sized by the reduction rate and the size of the pinion.

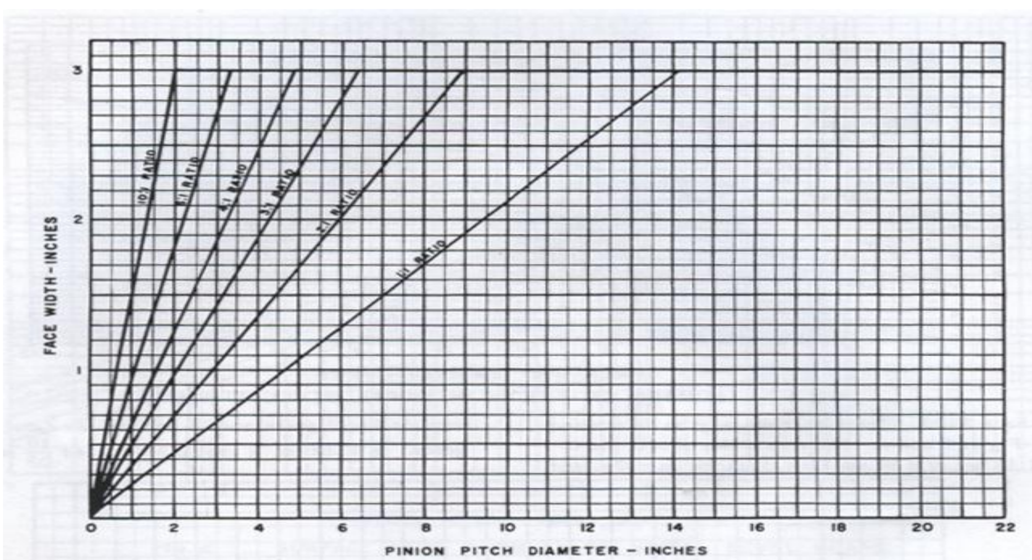

Figure 29. Face Width of Spiral Bevel Gear Based on Pinion Pitch Diameter

Face width was determined using the above graph with corresponding pitch diameter and reduction ratio. The face width of the driven gear is equal to that of the pinion for appropriate meshing.

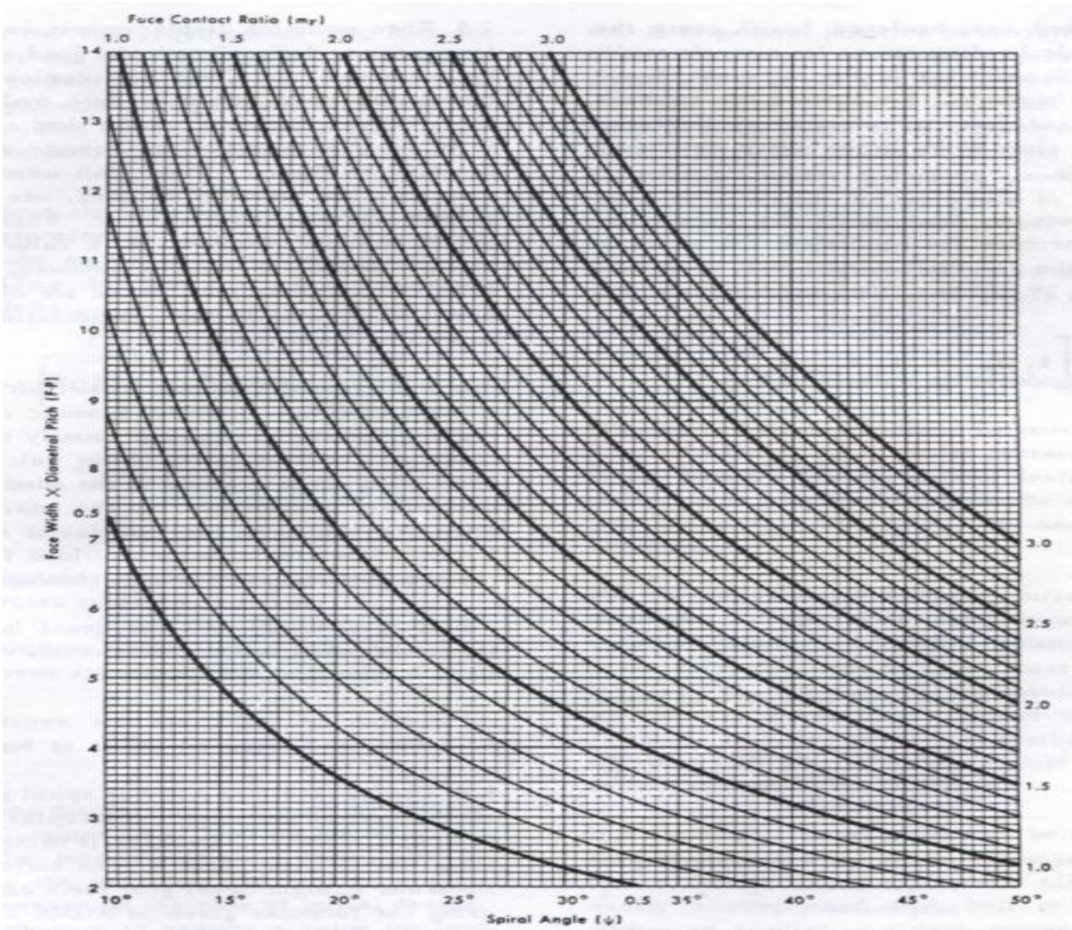

Figure 30. Spiral Angle Vs. Product of Face Width Times Diametral Pitch

	Pitch Diameter (inches)	Tooth count	Face width (inches)	Spiral angle (degrees)	Lifetime based on 5000 hrs (cycles)
Turn-box Pinion	2	17	0.7	35	2.4e9
Turn-box Gear	4	34	0.7	35	1.2e9
Combiner Pinion	2.3	17	0.8	37	1.2e9
Combiner Gear	4.6	34	0.8	37	1.8e9
Pusher Prop Gear	6.9	51	0.8	37	4.0e8

Table 4. Spiral Bevel Gear Sizes

The Planetary gear set was composed of the input sun gear two sets of five planetary gears and two ring gears. It was decided to use the carrier as the output to achieve our compound planetary shifting mechanism. The planetary gear shifts by locking up the primary ring gear. The primary is the ring gear in contact with the planets that directly contact the sun. An example is given in Figure 31. Diagram of Planetary Gear SetFigure 31.

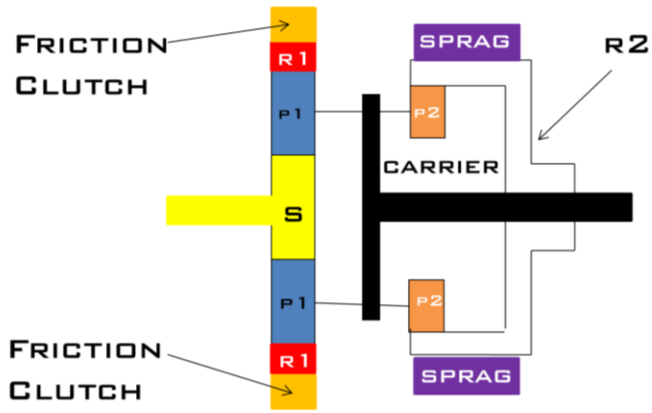

Figure 31. Diagram of Planetary Gear Set

When the primary gear is locked the lower reduction ratio is used giving the high-speed gearing the secondary ring gear is held by an overrunning sprag clutch, so this ring is nullified in the determination of the gear ratio and only the primary planetary matters. To shift to the low-speed output the clutch on the primary ring is released and the sprag clutch locks up and the higher gear reduction is now used. The planetary gear ratios and tooth count were determined with the help of Zihini B. Saribay a Ph.D candidate at The Pennsylvania State University. It was necessary to find ratios and tooth counts that were physically able to be made without planets interfering with one another. This is done with the following equation.

$$Possible\ combination\ if\colon \frac{N_{P1} + N_S}{Number\ of\ planets} = integer \qquad \text{Equation 17}$$

Equation for Planetary gears with no interference.

The physically recognizable ratio's that worked and tooth count are listed below.

5 Planets per ring	Sun	Planet 1	Ring 1	Planet 2	Ring 2
Tooth Count – N	22	18	58	14	64

Table 5. Planetary Gear Set Tooth count

The high and low speed output reductions were found using the following equations that were found in the AGMA standard 6123-A88.

$$\frac{N_S + N_{R1}}{N_{R1}} = 3.63 \qquad \text{Equation 18}$$

Reduction ratio for Single Planetary with: Sun - input, Ring 1- locked, Carrier – Output.

$$\frac{N_{P2} * N_S + N_{P1} * N_{R2}}{N_{P2} + N_S} = 5.03 \qquad \text{Equation 19}$$

Reduction ratio for compound Planetary with: Sun - input, Ring 1- free, Ring 2- locked, Carrier – Output.

After finding functional ratio's the physical size of the gears needed to be determined. This was done by first determining the critical gear in the planetary set. To determine which would be the critical gear plots of tooth loading vs. gear radius were created. The plot function were linked by picking a range of sizes for the sun gear and then relating the size of all the other gears in the set to the size of the sun gear based upon there ratios. The analysis proved the secondary planet gear to be the critical gear so the analysis from that point out on determining sizes was performed based on the secondary planet. It was also decided to use Helical Gears with a spiral angle of 25 degrees for the secondary ring and planet gears since they endure the highest stresses.

To determine the required gear sized the tooth bending stress equation was used to find values that matched up to materials allowable stress limit.

$$S_t = \frac{W_t K_a K_s K_m P_d}{K_v F J} \; lb/in^2 \qquad \text{Equation 20}$$

Equation for Bending Stress Number S_t.

$$S_t \leq \frac{S_{at} K_L}{K_T K_R} \qquad \text{Equation 21}$$

Equation for Determining Allowable Stress

The coefficients were determined from The Standard Handbook of Machine Design (Shigley, 1996) and are given in the table below. Coefficients listed as variables were dependent on radius and/or face width. An iterative program was designed to run through a series of the values and determine optimal gear sizing. The material used for making all spur gears, helical and straight, was chosen to be AISI 9310 CEVM steel. This material was chosen for its high strength to weight ratio which is optimal for aerospace design and this application. The given Allowable Bending Stress Number given below is for this material.

S_t	Bending Stress Number	Variable
W_t	Tooth Loading Force (lbs)	Variable
K_a	Application Factor	1.25
K_s	Size Factor for Bending Strength	1.0
K_m	Load Distribution Factor for Bending Strength	1.3
P_d	Diametral Pitch: ${Number\ teeth}/{Pitch\ Diameter}$	Vairable
K_v	Dynamic Factor for Bending Strength	0.9
F	Face Width (in)	Variable
J	Geometry Factor for Bending Strength	Use Reference
S_{at}	Allowable Bending Stress Number	65,000 lb/in^2
K_L	Life Factor for Bending Strength	1
K_T	Temperature Factor for Bending Strength	1
K_R	Reliability Factor for Bending Strength	1.5

Table 6. Coefficients for Determination of Bending Stress

From here an array of values for each gear were produced with varying gear radii, hence W_t , and F. Figure 32 shows the results of the array for the second planetary gear, the critical gear.

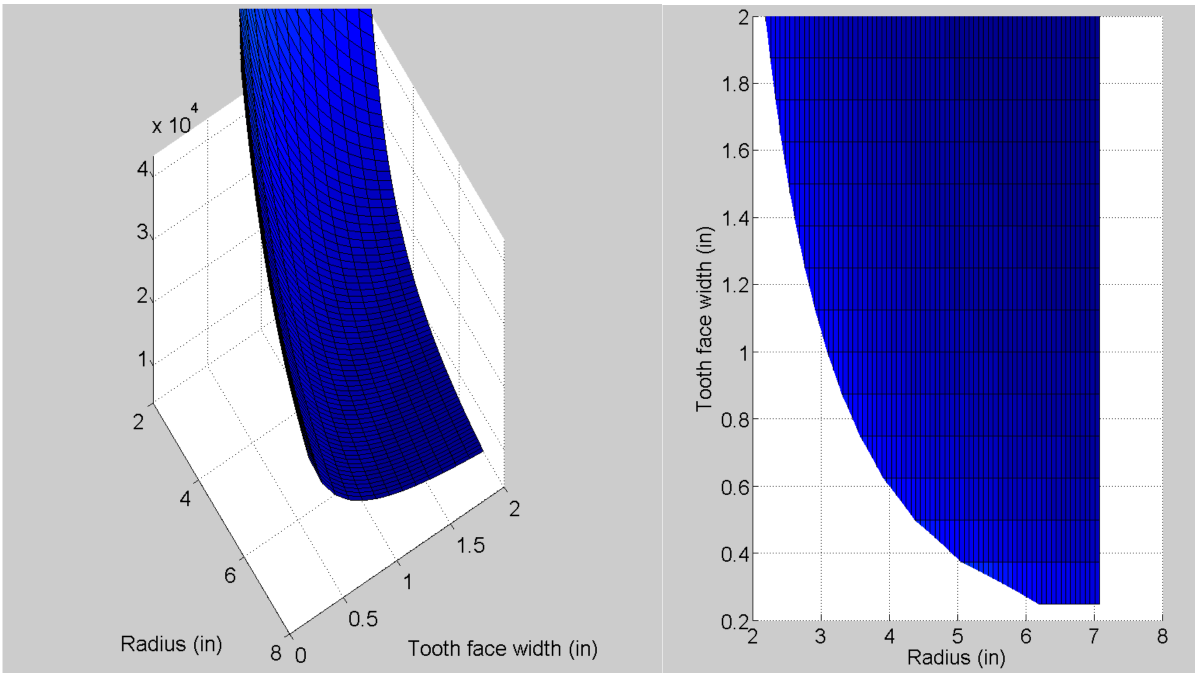

Figure 32. Second Planetary Bending Stress vs. Radius vs. Face Width

The three dimensional plot shows the relationship of face width and radius to tooth loading. There is a clear relationship that the larger the radius and larger the face width of the gear the lower bending stress it sees. The goal is to minimize weight with gears that can still carry the bending stress required. The two dimensional plot on the right shows the design space for tooth width and gear radius. In order optimize the design it was decided to look at face width and radius values that have a bending stress equal to or slightly less than equal to that of our design limit. This collection of design points can be seen in the 2-dimensional plot as the defining boundary to the left of the design space. The design points were then compared against one another with respect to the weight of the planetary transmission which can be seen in the figure below.

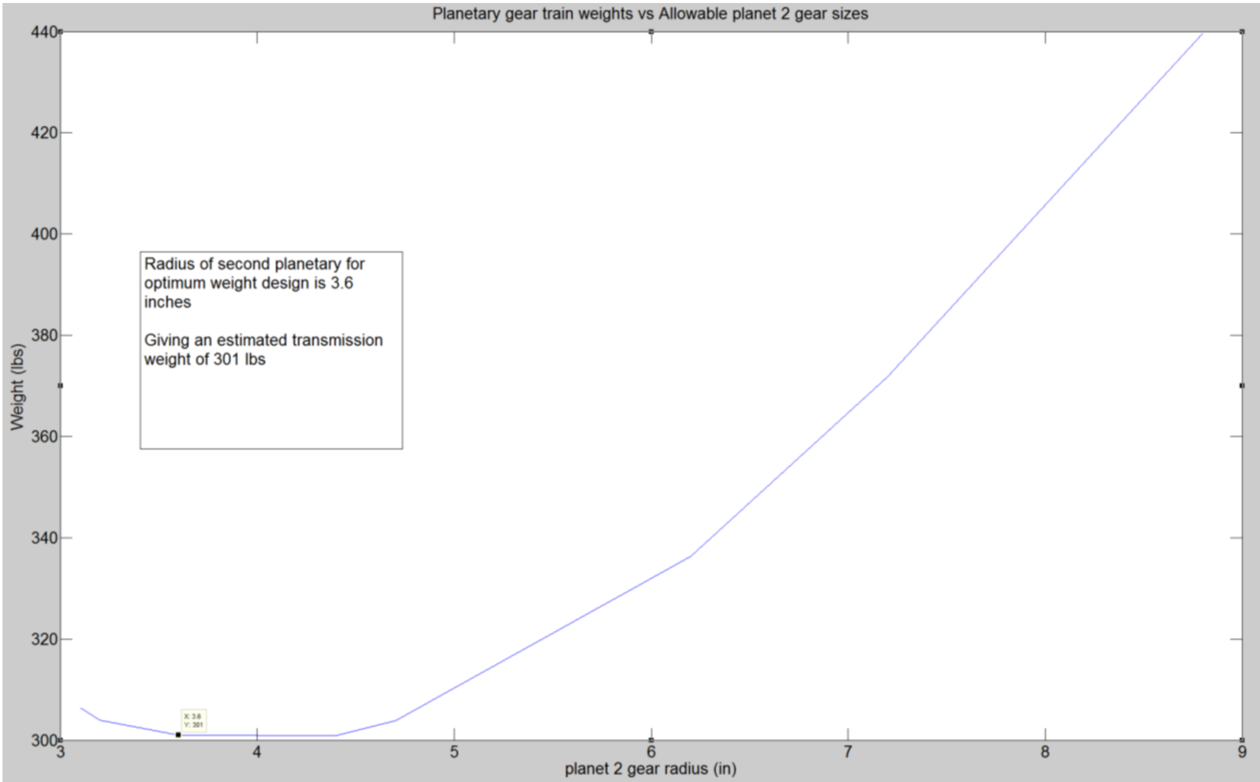

Figure 33. Planetary Gear Train Weight vs. Planet 2 Gear Radii at design points

The weight estimate was performed using the equation for the volume of a cylinder, were the radius is defined as half the pitch diameter and the height defined as the face width. The estimate also included a very crude estimate of the weight of the casing for the gear set because it was found initially that the larger the radius and thinner the width the lighter the gear set got however with the housing a parabolic curve was found as can be seen above. To minimize weight a design point that was a minimum along this curve was chosen for the gear sizing. These sizes were then all checked against each other for congruency to make sure the program had operated properly, which it did. The graph below shows the relationships between the radius of the secondary planet, the critical design gear, and the other gears in the planetary system. This is a generally high weight estimate to remain fairly conservative.

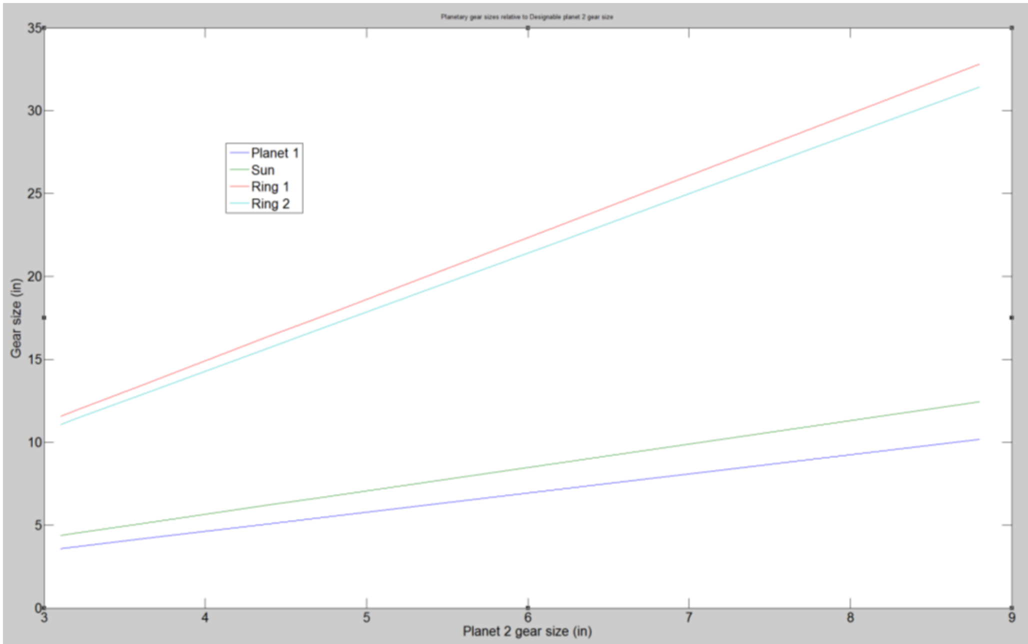

Figure 34. Gear Radii in Planetary vs. Radius of Second Planet Gear

It is clear that the second planet gear is the smallest not only from the fact that it is the critical gear due to highest tooth loading but also from the graph above which is based on the design geometry. Notice the ring gear sizes increase at the fastest rates. Physical dimensions of the transmission system are limited by the overall vehicle design as well, this was looked at after stress and weight analysis and determined not to be a problem. Table 7 lists the gear sizes that were determined from the program analysis with weight biasing.

At Face Width of – 1.5 in	Sun	Planet 1	Ring 1	Planet 2	Ring 2
Pitch Diameter (in)	10.16	8.32	26.82	7.2	25.7

Table 7. Planetary Gear sizes

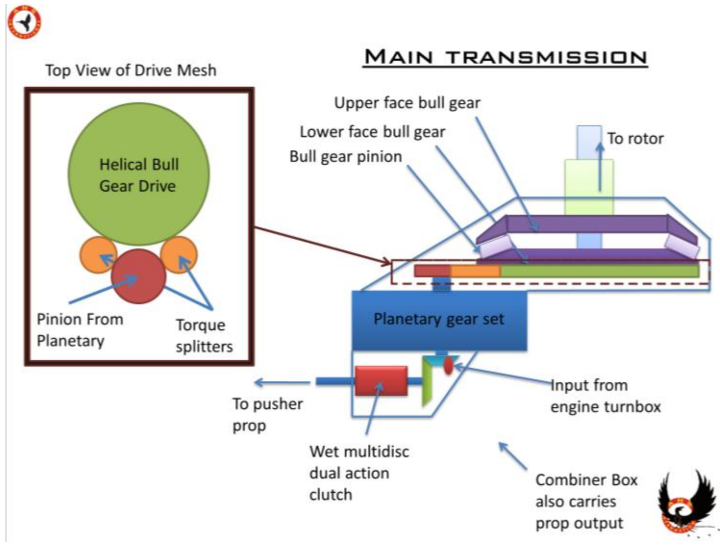

Figure 35. Main Transmission Layout

The output shaft of the planetary which is connected to the carrier is directly connected to the next helical gear which meshes with two more helical gears with a reduction ratio of 1.5:1. Those two helical gears then mesh with the lower bull gear on its outer edge and drive the rotor system with a reduction of 3.33:1. The lower bull gear drives the upper bull gear with a face gear meshed with 4 Idler/Accessory drive gears which then mesh with the upper bull gear also giving it the counter-rotation required. The gear sizes are given in Table 8.

	Tooth Count	Pitch Diameter (in)	Face width (in)
Pinion from planetary	30	15	2.5
Torque splitters	20	10	2.5
Lower Bull Gear (Outer helical cut)	100	50	2.5
Lower Bull Gear (Face Gear)	100	48.5	3
Idler/Accessory drives	10	2.5	3.5
Upper Bull Gear (Face Gear)	100	48.5	3

Table 8. Bull Gear, Bull Gear Drivers, Idler and Accessory Drives

Pusher Prop

The pusher prop was designed using online software called JavaProp (Hepperle, 2003). It uses blade element theory. The blades are cut into small pieces along the radius. At each location, the program uses the local airfoil selected and blade angle to do the calculations for that piece. All the pieces are combined to get the velocity added to the flow from the propeller which leads to the thrust provided.

This software allows the user to pick an airfoil at four different locations along the blade. From there, angle of attack of each section can be selected. Once the blade is designed, number of blades, rotation speed, diameter, spinner diameter, operation velocity, and thrust required can be selected. Once all those are selected, the program can be run and efficiency is provided. Since the pusher prop is most needed at the high speed, it was decided to optimize the prop at the upper range of the operational window. In order to get the best efficiency, all the above variables were altered and iterations were done to find the optimum design. Once the design of the pusher prop was optimized for the higher speed case, new velocity and thrust requirements were entered, and the collective pitch of all the blades were changed to find the new best efficiency.

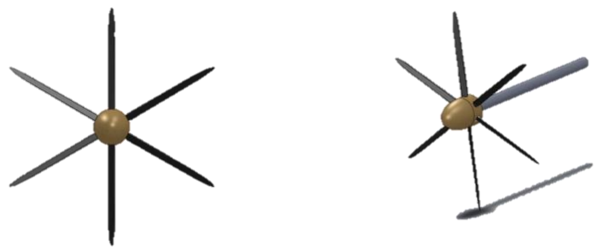

Figure 36. Pusher Propeller Design Images

After doing the design process, a 5 ft radius pusher prop was used spinning at 3,500 RPM. The inner quarter of the blade uses a MH 112 airfoil, the middle half uses a MH114 airfoil, and the outer quarter uses a MH 116 airfoil. The twist of each blade went from one degree at the root to seven degrees at the tip. The chord of each blade is 0.25 ft. The graph below shows the how the efficiency changes over the operational speed.

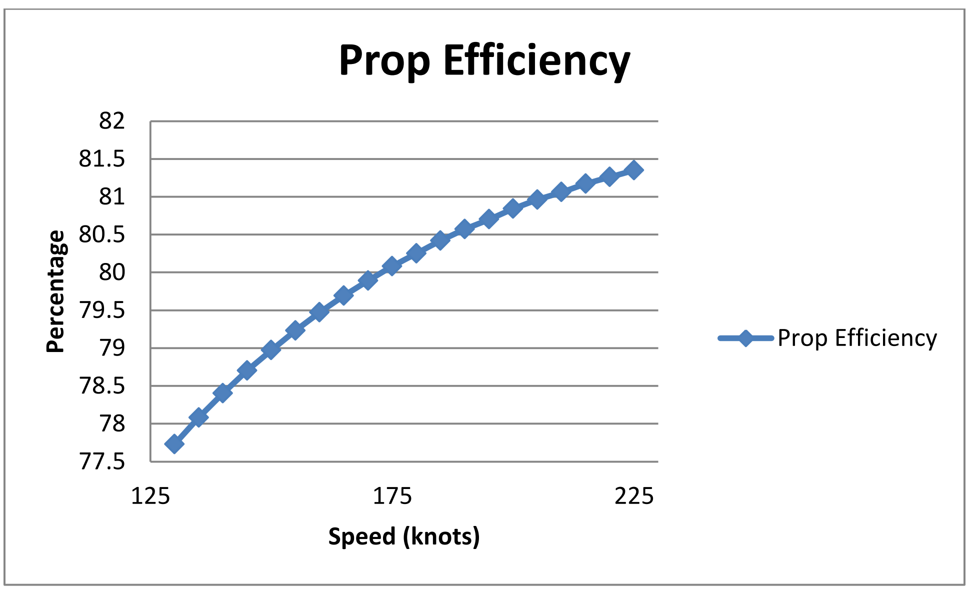

Figure 37. Propeller Efficiency over a Range of Speeds in Knots

In order to validate that JavaProp actually matched real life data, the publisher of the software compared data from NACA Technical Report 594 with predicted values from the software. The two sets of information match within reason in the operational range of the prop. Only at the very low speeds was there a big difference between the two. Those speeds are only seen for a very short time at take-off and landing of a conventional prop aircraft, and not seen at all on this helicopter since the pusher prop is only used at higher speeds when it is needed.

Systems

Communication for the helicopter will use both a VHF radio and satellite for safety. Both systems will come from Honeywell. The radio will be the KTR 908. It has a very wide range of frequencies and automatic audio leveling for ease of use. The satellite communication will be MCS-7163, which is a basic satellite communication system.

Navigation will also use two systems for safety. Honeywell's KNR 624A VOR will be used for land based navigation as well as Northrop Grumman's LN-270 GPS. Using the two systems will provide the pilot with multiple systems to determine location and heading in case one fails or isn't picking up a signal.

Weather, terrain, traffic, and lightning warnings will all be provided by Honeywell's MFRD system. By having all the warnings coming from one system, the pilot will know exactly where to look when an alert is sent.

In order to provide the pilot and maintenance workers information about the health of the vehicle, BAE Systems' HUMS will be installed. The system monitors critical areas of the helicopter and will inform the pilot if a flaw is beginning to occur. This can also save time for maintenance workers. Instead of having to do complete checks of the entire aircraft, the HUMS will tell them where parts are beginning to fail.

Back-up power to the helicopter will be provided by a Honeywell 331-250 APU. This APU provides 90 kW of electrical power, which will be more than enough to cover all the systems on board the helicopter.

To provide safety to the crew, crashworthy seats will be placed in all the permanent seat locations. For this, Goodrich A2C2S seats will be used. The seat strokes in the event of a crash while dissipates the energy before it reaches the spine of the person in the seat. Many seats require users to dial in their weight which will adjust the resistance of stoking mechanism. This can be complicated to know when caring a bunch of equipment. This seat doesn't require users to know their weight, providing confidence that the seat will prevent injury in the event of a crash.

Environmental controls for the aircraft will be split between the cockpit and cabin. This will be done to keep the pilot and co-pilot comfortable when the crew is working with the door open. The pilot and co-pilot will both be equipped with BAE Systems Air Warrior. In addition to providing bullet protection, Air Warrior has a direct hose to the vest that allows for adjustable air temperatures. Since the system sends the cool air directly to the wearer, there is little loss to the outside air. Air Warrior can only be used for the pilot and co-pilot because they are stationary during the entire mission. For the cabin where passengers will be moving around, a Honeywell Air& Thermal Management System will be used. This system will control the air flow and temperature into the cabin to keep the passengers comfortable. Since the temperature will change greatly between door open and door closed situations, this system monitors the temperature and will adjust based on readings.

During the search and rescue mission, a hoist will be required to bring the person aboard the helicopter. For this, the Goodrich 42305-R hoist will be used. This hoist is mounted inside the cabin and swings out in order to be used. By not having the hoist mounted on the outside of the helicopter, there is no additional drag on the aircraft. This was important so the performance of the aircraft wasn't brought down. The hoist has 250 ft. of line with a lift load of 600 lbs. and an ultimate load of 2,700 lbs. The hoist also has a quick installation and removal process, so it can easily be removed for missions where it isn't needed.

In order to provide military missions with additional safety over civil missions, a few additional systems will be added to that version. To navigate poor weather conditions or night time, a forward looking infrared system will be installed. Night vision is blinded by fog, rain, dust, and other poor visibility environments. Forward looking infrared simply uses heat to build a map for the pilot to use in order to navigate. Also useful in military settings is the fact that infrared doesn't send out a signal like radar. Not sending out a radar signal is one less tool for an enemy to use in order to locate the helicopter. The infrared system used will be from FLIR, and company who specializes in infrared systems.

Also on the military version will be a missile approach warning system. This alerts the pilot when someone has launched a missile at the helicopter and it has locked on. From there, the pilot can either take evasive actions or launch countermeasures. The countermeasures involve chaff and flares. The chaff involves releasing a large amount of small aluminum pieces in the air to create a large cloud around the helicopter to hide from missiles using radar. In order to overcome heat seeking missiles, the flares will be used. The flares released are at a higher temperature than the engine in order to get the missile to lock on to a different target. Both the missile warning system and countermeasures will be from BAE Systems. AN/AAR-57 is the missile warning system and ALE-47 is the countermeasure system.

IR Suppression

Infrared suppression on the helicopter will be done by mixing downwash from the main rotor with the engine exhaust air. The two will be combined in ducting within the helicopter to allow for it to mix and bring the engine exhaust temperature down. Once the air moved through the ducting, it will be exhausted out the side of the helicopter out a long, thin exhaust duct. Spreading the exhaust over a large area prevents a plume from building up behind the helicopter. As the helicopter moves through the air, the large exhaust area makes it so the exhaust is blown away quickly. The size of the inlet for the downwash will be determined based on the exhaust temperature requirements and how much downwash air is required to bring the engine exhaust down to that temperature. Figure 38 shows the air flow path for the IR suppression.

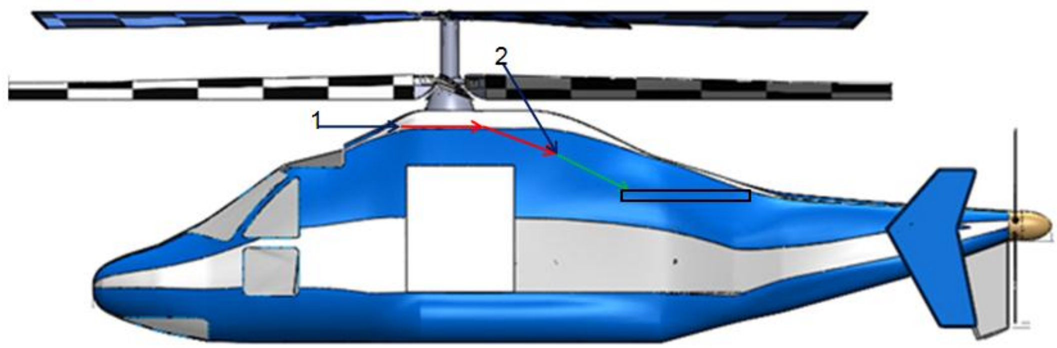

Figure 38. IR Suppression System Location

In Figure 38, path 1 is the engine intake. Initially at ambient temperature (blue), it becomes hot (red) as it moves through the engine. Path 2 is the downwash coming from the rotor and being mixed with the engine exhaust. The green line shows the temperature between the hot engine exhaust and the cool ambient air moving to the long, thin vent area where it is sent back out into the free stream.

Flight Controls

The helicopter will use a fly-by-wire flight control system. This was chosen because it is easy to make the system triple redundant for safety. The stick inputs will be processed by the computer, which will then control hydraulic pumps that will move the control surfaces. It was decided to use hydraulic pumps over electrical actuators because of the force required to move the control surfaces. It was deemed that the electrical actuators would become too big and heavy to try and have any form of weight savings.

Noise

Several design features of the helicopter also help reduce the noise signature. By lowering the rotor RPM at high speeds, the impulsive noise of the helicopter is reduced. Lowering the blade speed prevents the tip of the blade from seeing transonic flow, which can cause a lot of noise in addition to the performance penalty. Using the co-axial design with a total of eight blades also helps lower the blade loading noise of the aircraft. Having eight blades compared to three or four of a conventional helicopter lowers the total force each blade must produce, which will lower the blade loading noise.

Also helping trim down the noise produced is the housing design used on the engine. The engine is mounted inside the airframe and with the addition of placing dampening pads between the skin and engine will make it harder for the noise to escape out to the atmosphere where it can be heard.

Mission

Fuel Analysis

A fuel analysis for each of the three missions was performed to estimate the size of the internal tanks of the Phoenix. In order to accurately estimate the fuel usage, a minute by minute analysis of each mission was performed. Each mission was broken into specific performance requirements by AHS in the figure below. Each of the segments has different operating conditions in which the Phoenix's engine performance and power requirements change. The fuel analysis calculates the power required at each flight regime, the power available at each regime and the amount of fuel burned each minute during the mission while adjusting the total weight of the aircraft throughout the mission accounting for the fuel burn. The standard CT7-8A was chosen and not scaled up or down.

The CT7-8A specific fuel consumption at max takeoff power is 0.45. The power available at each of the flight conditions was found using eqn. 22, 23 and 24 (Leishman, 2006).

$$Power_{alt} = Power\left(\frac{\delta}{\theta}\right) \quad \text{Equation 22}$$

$$\delta = \left(\frac{Pressure_{alt}}{Pressure_{Std}}\right) \quad \text{Equation 23}$$

$$\theta = \left(\frac{Temp_{alt}}{Temp_{Std}}\right) \quad \text{Equation 24}$$

	Mission 1	Mission 2	Mission 3
Title	Search and Rescue	Insertion	Resupply
Start up/Warm Up	5 minutes	5 minutes	5 minutes
6K95 HOGE	1 minute	1 minute	1 minute
Climb	Best Altitude	Best Altitude	Best Altitude
Outbound Leg	225 nm @ V br	250 nm @ V br	250 nm @ V br
Descent	To Search Altitude	To 6K95 HOGE	To 6K95 HOGE
Loiter	30 minutes @ V be	N/A	N/A
Descent	To 6K95 HOGE	N/A	N/A
6K95 HOGE	5 minutes	N/A	N/A
6K95 Landing	N/A	1 minute	1 minute
Unload (Hot) /Load (Hot)	N/A	10 minutes	20 minutes
6K95 HOGE	N/A	1 minute	1 minute
Climb	To Best altitude	To Best Altitude	To Best Altitude
Inbound Leg	225 nm @ V mcp for 50 to 70 minutes	250 nm @ V br	250 nm @ V br
Descent	To 6K95 HOGE	To 6K95 HOGE	To 6K95 HOGE
6K95 HOGE	1 minute	1 minute	1 minute
Landing / Cool Down / Shutdown	5 minutes	5 minutes	5 minutes

Figure 39. Mission Break Downs for Minute by Minute Analysis Given by AHS RFP

The pressures and temperatures at each flight condition are as follows:

- Start-up/Warm-up
  - Represents a Landing Strip during summer Afghanistan day
  - 3000 ft. pressure alt
  - 115°F
- 6K95 HOGE
  - 6000 ft. pressure alt

- 95°F

- Best Altitude, Climb, Outbound/Inbound Legs,
  - 9000 ft. pressure alt
  - 93°F
  - Based on landing strip conditions
- Search Alt
  - 3800 ft. pressure alt
  - 112°F
  - Based on landing strip conditions

The pressure and temperatures based on each flight condition change the maximum continuous available power of the CT7-8A. The maximum continuous power at standard day conditions is 2043 horsepower per engine. The Phoenix with two engines has 4046 HP available during standard conditions, 3560 HP on the Afghan landing strip, 3358 HP at 6K95, 3003 HP at cruise and 3482 HP at search alt.

Each of the leg of the mission occurs at different velocities and thus different horsepower which are best illustrated below for each mission.

Mission I Search and Rescue

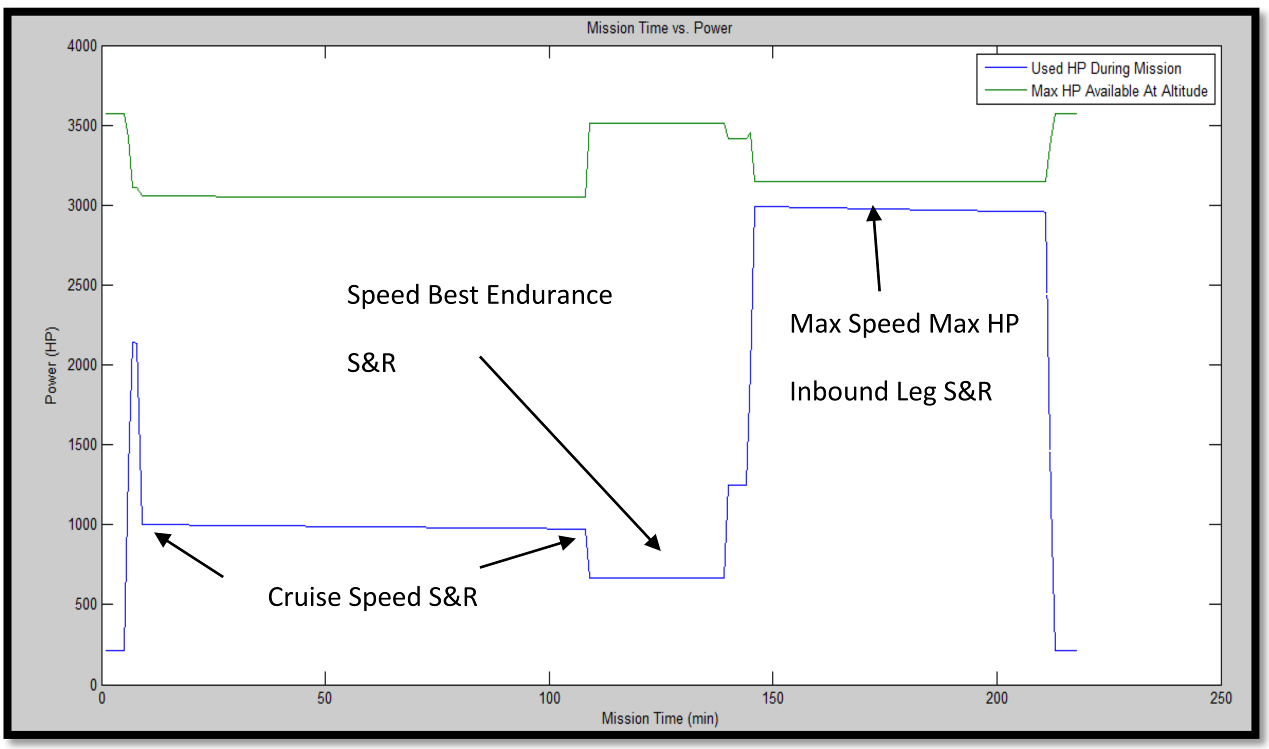

Figure 40. Mission 1 Power Used and Power Available vs. Mission Time

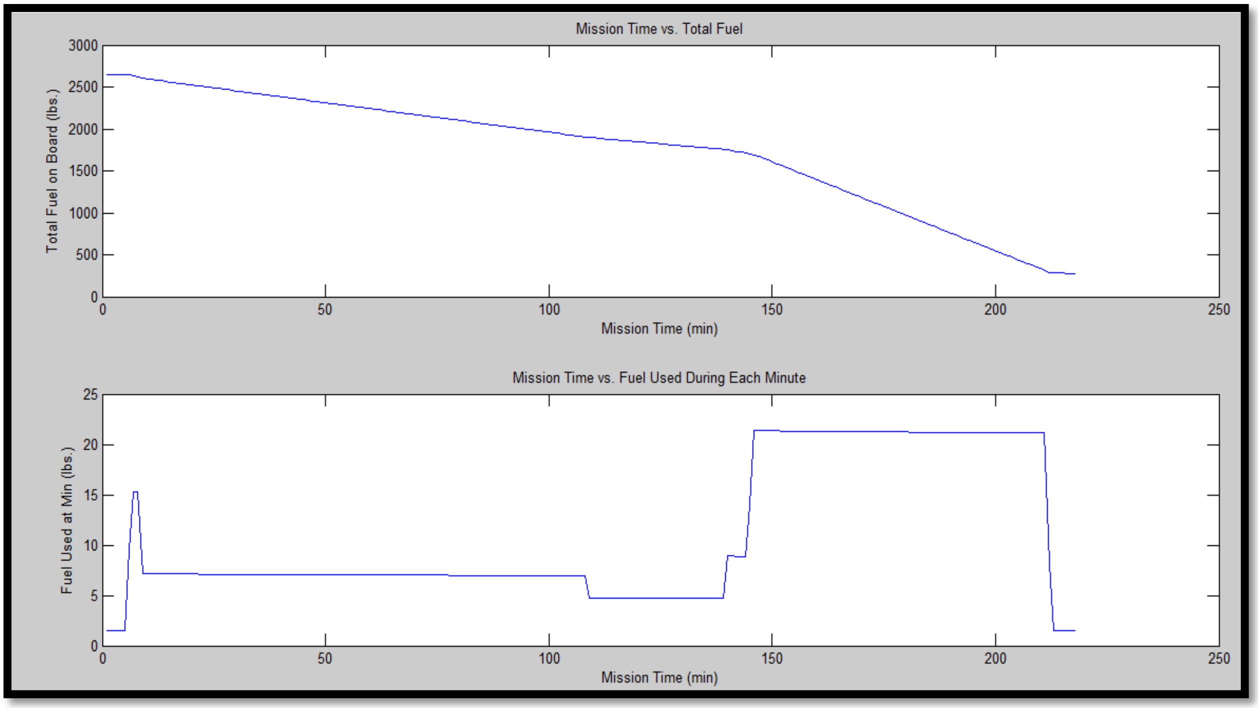

Figure 41. Mission 1 Fuel on Board vs. Mission Time (Top) Fuel Used in Pounds vs. Mission Time (Bottom)

Mission II Insertion

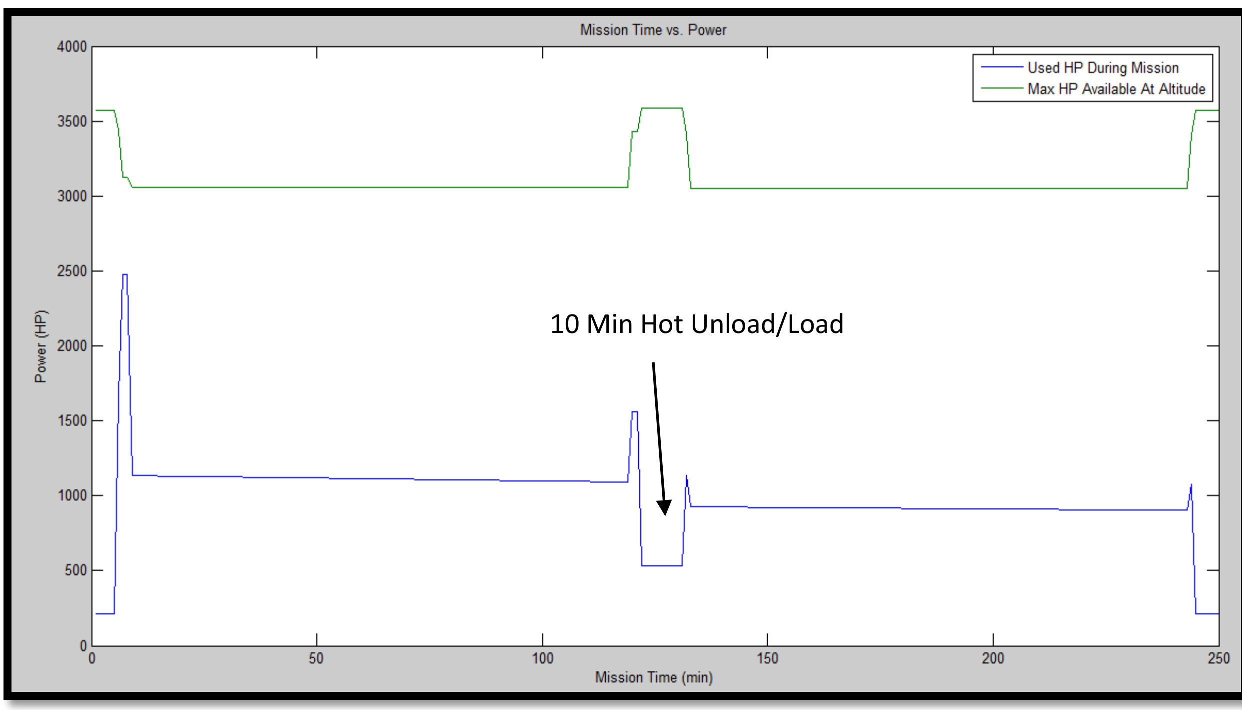

Figure 42. Mission 2 Power Used and Power Available vs. Mission Time

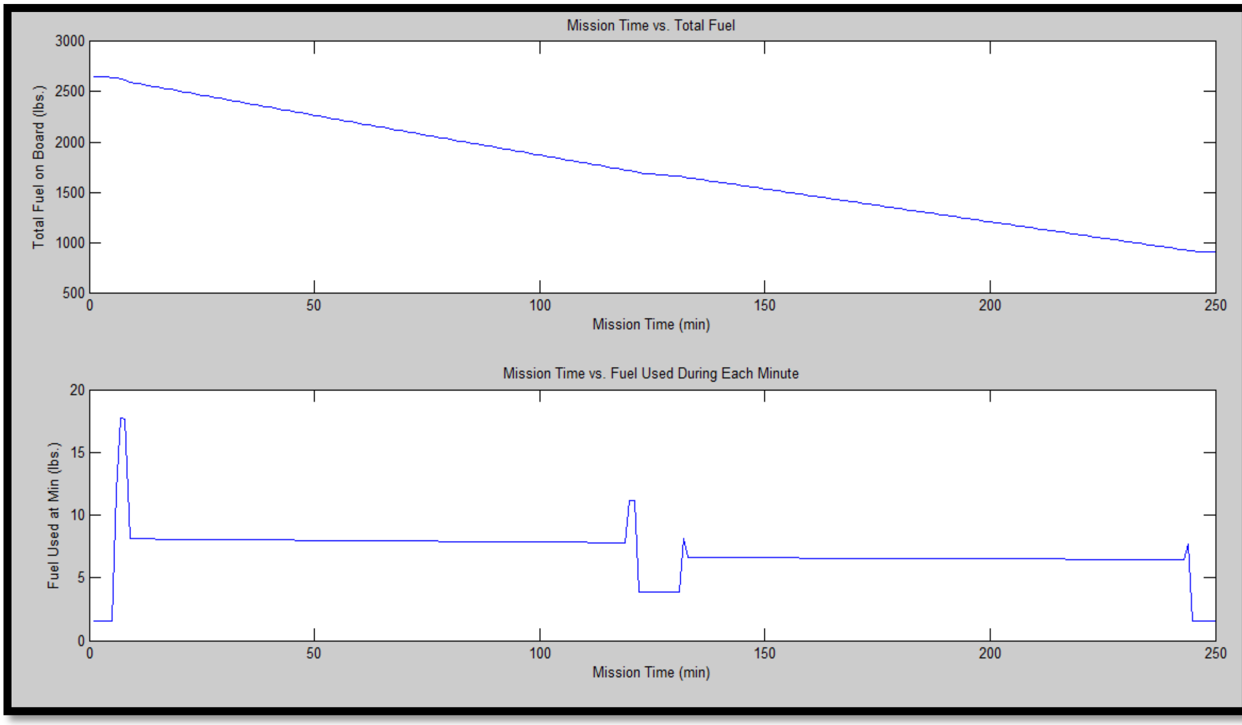

Figure 43. Mission 2 Fuel on Board vs. Mission Time (Top) Fuel Used in Pounds vs. Mission Time (Bottom)

Mission III Resupply

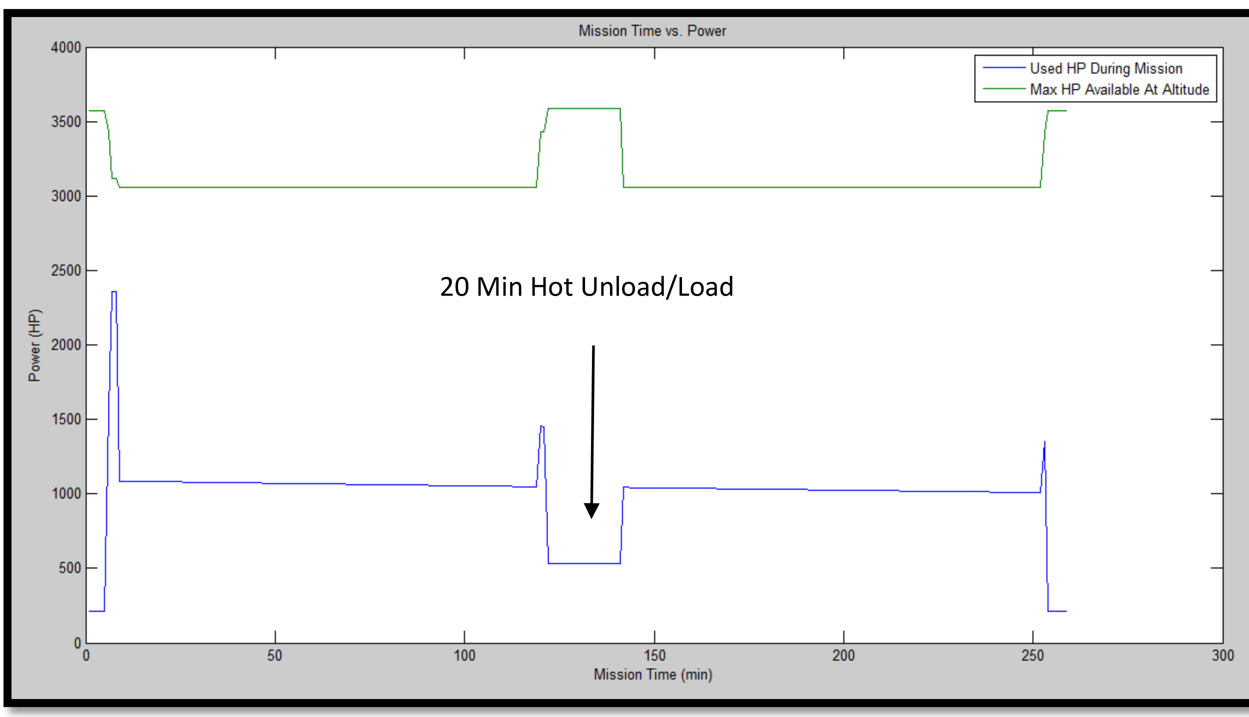

Figure 44. Mission 3 Power Used and Power Available vs. Mission Time

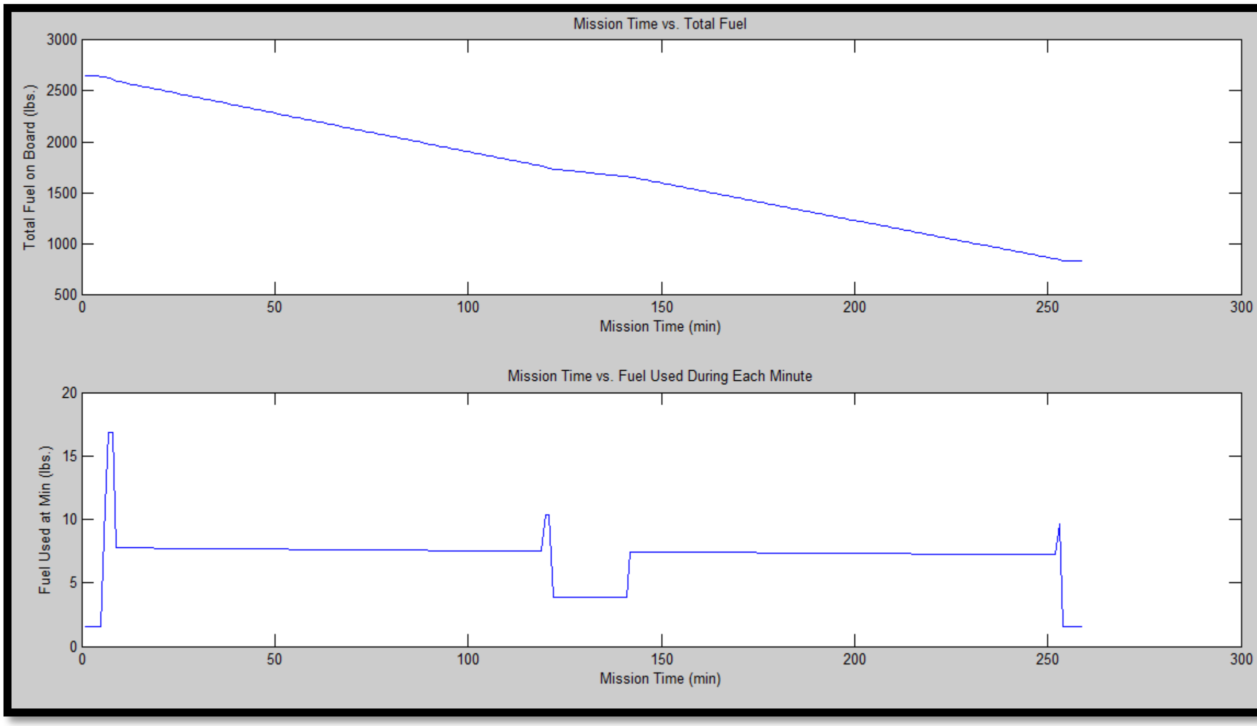

Figure 45. Mission 3Fuel on Board vs. Mission Time (Top) Fuel Used in Pounds vs. Mission Time (Bottom)

Fuel Summary

The total amount of fuel required for the completion of mission with a 10% reserve left is 2650 lbs of fuel. This roughly translates into 395 gallons. This amount was increased from the rough calculations of 2500 lbs of fuel in the weight analysis. This was done because the search and rescue mission was initially done with the golden hour taking the maximum amount of time of 70 min. It was found however, that there was still some power left over at cruise altitude. The speed was then increased to 210 knots on the inbound leg to use all the available power possible in order to get the patient back as fast as possible. The increase in speed then led to an increase in power and fuel consumption. The tanks had to be enlarged to still have enough fuel plus reserves to accommodate the increase in speed.

	Mission I	Mission II	Mission III
Duration(min)	219	250	260
Fuel Used(lbs)	2376	1748	1828
Fuel Unused(lbs)	274	902	822

Table 9. Mission Times, Fuel Used and Fuel Left over at Mission End

Weight Analysis

The gross weight was calculated using an estimate published by Raymond Prouty (Prouty, 1995). A gross weight has to be assumed for this analysis and a weight of 16000 pounds was selected. Estimating that a helicopter could lift just over half its weight and using a lifting weight of 5000 pounds. The helicopter should be 9000 pounds empty plus 4000 for the cargo, 1000 pounds for pilots and crew and a rough calculation of fuel around 2000 pounds makes a rough estimate of 16000 pounds.

Using the gross weight estimate and basic values found earlier a program can be written to more accurately calculate the weight. The program uses the following equations to estimate each part of the platform.

Main Rotor Blades = 1600 lbs.

$$W_{Blades} = 0.026(Number\ of\ Blades^{0.66})cR^{1.3}(\Omega R)^{0.67} \quad \text{Equation 25}$$

The main rotor blade weight was calculated using one of the two main rotors. This was done because Prouty's calculations are based off a conventional helicopter. The number of blades per rotor is four. The chord is 2.12 ft. and the rotor has a radius of 22.5 ft. In order to maximize the weight of the blades the greatest rotor velocity was chosen, Ω=30.2 rad/s. Using these values each blade weighs 165 pounds. An additional 35 pounds was added to each blade to account for the increased rigidity of the entire rotor system. The total weight of each rotor blade is 200 pounds. The total co-axial rotor system consists of two main rotors hence the total main rotor blade weight is 800lbs.

Main Rotor Hub = 750 lbs.

$$W_{Hub} = 0.0037(Number\ of\ Blades^{0.28})R^{1.5}(\Omega R)^{0.43}\left(0.67W_{Blades} + \frac{gJ}{R^2}\right) \quad \text{Equation 26}$$

$$Where\ J = \left(\frac{W_{Blades}}{g}\right)\left(\frac{R}{2}\right)^2 (Number\ of\ Blades) \quad \text{Equation 27}$$

Using the values to calculate the weight of the rotor blades the main rotor hub weight can be calculated. The Main Rotor hub weighs 350 pounds and again this value is multiplied by 2.

Horizontal Stabilizer = 85 lbs.

$$W_{HStable} = 0.72(AreaHorizontalStablizer^{1.2})(AspectRatioHorizontalStablizer)^{0.32} \quad \text{Equation 28}$$

A stabilizer analysis was conducted and the size and shape of the stabilizer was determined using a trend analysis. The horizontal stabilizer area was determined to be 40.5 ft^2 with an aspect ratio of 2.75.

Vertical Stabilizer = 90 lbs.

$$W_{VStable} = 1.05(AreaV.Stab.^{0.94})(AspectRatioV.Stab.)^{0.53}(\#\ of\ Tail\ Gear\ Boxes)^{0.71} \quad \text{Equation 29}$$

The vertical stabilizer is made up of three different surfaces in three different locations. Two of the vertical tail surfaces are located on the ends of the horizontal stabilizer forming an H-tail configuration. The third vertical tail surface also serves as a prop guard and third wheel landing gear. The H-tail ends each weigh 25 lbs. and the prop guard weighs 40 lbs. for a total of 90 lbs.

Pusher Rotor = 100 lbs.

$$W_{Pusher} = 1.4(Radius\ Pusher)^{0.9}\left(\frac{Transmission\ HP\ Rating}{\Omega}\right)^{0.90} \quad \text{Equation 30}$$

The weight of the pusher was estimated by using a 4ft radius, a 3000HP XMSN and an omega of 30.2.

Body = 2000 lbs.

$$W_{Fuselage} = 6.9\left(\frac{GW}{1000}\right)^{0.49} LengthFuselage^{0.61}(S_{Wet})^{0.25}$$ Equation 31

The body was calculated using the estimated GW of 16000lbs, a length of 46.5 feet and the wetted area of 2500 ft^2.

Landing Gear = 370 lbs.

$$W_{LG} = 40\left(\frac{GW}{1000}\right)^{0.67} (No.of\ Landing\ Gears)^{0.54}$$ Equation 32

Engine Weight = 1250 lbs.

$$W_{Engines} = (\#\ of\ Engines)(Installed\ Engine\ Weight)$$ Equation 33

$$Where\ No.of\ Engines = 2$$

$$Installed\ Engine\ Weight\ of\ CT7{:}\ 540\ pounds$$

The CT7-8A weighs about 540 lbs. 35 lbs. of fluids and 50 lbs. of subsystems and hookups have been added totaling 625 lbs. The Phoenix has two CT7-8A engines installed.

Fuel Weight = 2650 lbs.

$$W_{Fuel} = 2650\ pounds$$

Drive System Weight = 1340 lbs.

$$W_{Drive} = 13.6(Transmission\ HP\ Rating)^{0.82}\left(\frac{RPM}{1000}\right)^{0.037} \times \left(\frac{No.of\ Gearboxes^{0.066}}{\Omega\ Main^{0.64}}\right)$$ Equation 34

The drive system was estimated using a 3000 HP XMSN rating and 4 gears boxes with the same main rotor rotation rate, omega 30.2 rad/s.

Cockpit Control Weight = 250 lbs.

$$W_{CC} = 11.5\left(\frac{GW}{1000}\right)^{0.40}$$ Equation 35

Instruments Weight = 130 lbs.

$$W_{Instruments} = 3.5\left(\frac{GW}{1000}\right)^{1.3}$$ Equation 36

Misc. Weight (Hyd. & Elec.) = 250 lbs.

Avionics Weight = 400 lbs.

Furnishings and Equipment Weight = 200 lbs.

Vibration Control = 300 lbs.

The empty calculated weight of the Phoenix is 9115 lbs. without fuel. In the fully loaded condition with fuel, the heaviest predicted load and crew is 16415 lbs.

CG

The center of gravity was calculated using the above weights. Each major components position was estimated and the CG was found by using a simple moment arm calculation. Below is Figure 46 showing the position that each major component acts with the CG.

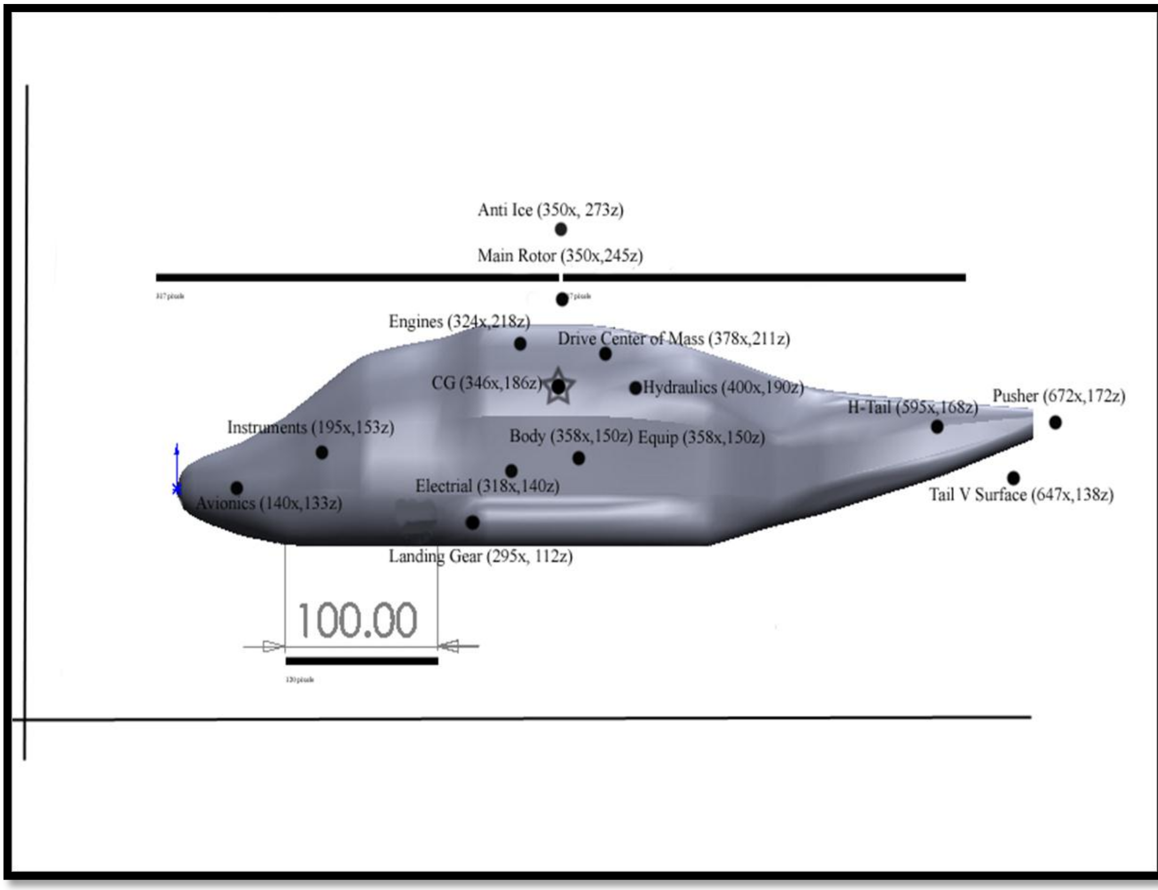

Figure 46. CG Position with Major Components Plotted

The CG in relation to Main Rotor

- 4 inches in front, 60 inches under

CG in relation to Pusher

- 14 Above, 27 in front

Adding Fuel Brings CG Down 10 inches and moves back 1 in

CG in relation to Main Rotor

- 3 inches in front, 70 inches under

CG in relation to Pusher

- 4 Above, 27ft in front

Cost Analysis

A projected hourly and acquisition cost of the Phoenix was obtained using existing helicopter platforms operated by the United State Army and Marine Corps. Nine different platforms including the CH-47, V-22, and CH-53E were plotting using installed horse power vs. hourly operating cost to obtain a base operating cost of the platform.

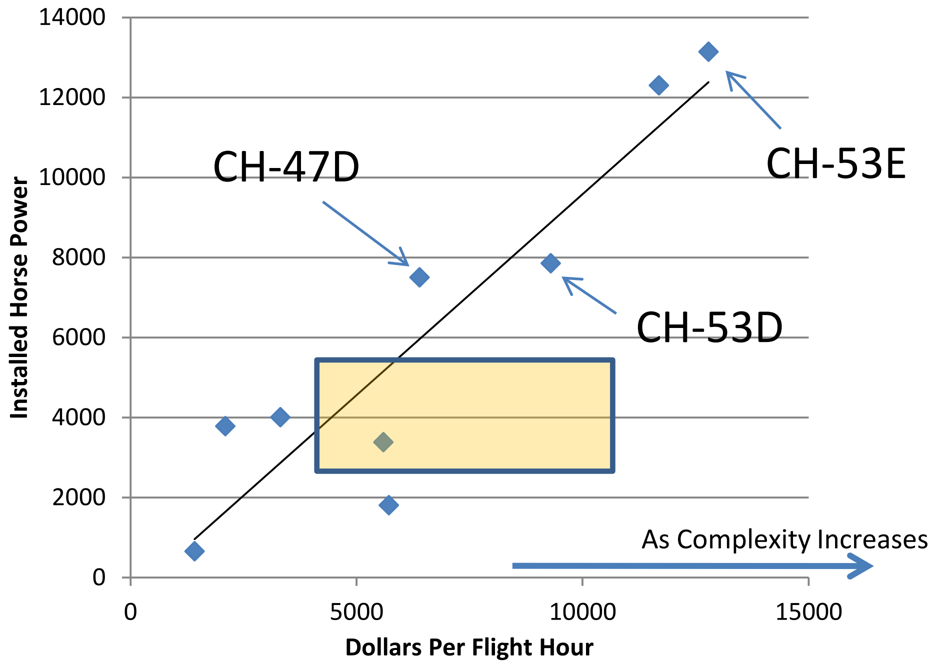

Figure 47. Basic Platform Cost vs. Installed Horsepower w/ Phoenix Cost Range

A conservative base hourly cost of $4800 was obtained per the installed horsepower onboard the Phoenix. Fuel was then factored out of this base cost and the resulting hourly cost was $4500. This base cost was then chosen to represent 3 basic expenses; the main rotor, the engines/drive and other miscellaneous items. Using the base cost of $1500 for each of these components a projected hourly cost is obtained. If one main rotor costs $1500 per hour on more conventional rotorcraft with 4000 horsepower then it stands that a co-axial rotor system will cost twice that, resulting in $3000 plus the maintenance of a "smaller rotor" or pusher prop at 75% the cost of a main rotor $1125. The engines overhaul and maintenance will become increasing complex with the additional co-axial and pusher prop systems, resulting in $3000 for the engines and the miscellaneous items were deemed to remain the same at $1500. The total projected hourly cost with acquisition cost factored in is $3000+$3000+$1125+$1500= $8625. Assuming the acquisition cost of 1000 dollars per flight hour over a total of 10000 hours per airframe the acquisition cost of each Phoenix platform is 10 million dollars with a projected hourly operating cost of $7625 per hour.

Nomenclature

"	Inches
°C	Celsius
°F	Fahrenheit
3G	Three times the Force of Gravity
6K95	A density requirement set in the RFP
a	Airfoil Lift Curve Slope
AGMA	American Gear Manufacturers Association
APU	Auxiliary Power Unit
BE	Blade Element
c	Blade Chord
CG	Center of Gravity
C_{Do}	Profile Drag Coefficient
C_{T1}, C_{T2}	Thrust Coefficients
D_f	Fuselage Drag
DL	Disk Loading
f	flat plate area
F	Face Width (in)
f_{aux}	Percentage of Helicopter Flat Plate Area
ft	Feet
ft/s	Feet per Second
g	Gravity
GPS	Global Positioning System
H	Rotor Rolling Moment
h_{cg}	Center of Gravity Below Main Rotor
hp	Horsepower
HUMS	Health and Usage Monitoring System
IR	Infrared
J	Geometry Factor for Bending Strength
K_a	Application Factor
K_L	Life Factor for Bending Strength
K_m	Load Distribution Factor for Bending Strength
K_R	Reliability for Bending Strength
K_s	Size Factor for Bending Strength
ksi	Kilopound per Square Inch
K_T	Temperature Factor for Bending Strength
kts	Knots
K_v	Dynamic Factor for Bending Strength
k_x, k_y	Inflow Gradients
L/D	Lift over Drag
lb/in_3	Pound per Cubic Inch
lbf*ft	Pound Feet
lbf*ft/min	Pound Feet per Minute
lbs	Pounds
lbs/ft^2	Pound per Square Feet
L_f	Fuselage Download
MATLAB	Matrix Laboratory R2010a
M_{dd}	Airfoil Drag Divergence Mach number
MS	Microsoft
$M_{tip,adv}$	Advancing Tip Mach Number
M_y	Rotor Pitching Moment
nm	Nautical Miles
N-m	Newton Meters
NOTAR	No Tail Rotor Helicopter Anti-Torque System
Pd	Diametral Pitch: Number of Teeth/Pitch Diameter
psi	Pound per Square Inch
Q	Torque
R	Rotor Radius
rad/min	Radians per Minute
rad/s	Radians per Second
RFP	Request For Proposal
rpm	Revolutions per Minute
Sat	Allowable Bending Stress Number
sl/ft^3	Slugs per Cubic Feet
S_r	Rotor Spacing
St	Bending Stress Number
T	Thrust
T_{aux}	Auxiliary Thrust
v	Velocity
V_∞	Reduction Velocity
VHF	Very High Frequency
VOR	Voice Operated Recording
$V_{tip,adv}$	Advancing Tip Speed
W	Gross Weight
w/	with
W_{blades}	Blade Weight
W_{CC}	Cockpit Controls Weight

W_{drive}	Drive System Weight
$W_{engines}$	Engine Weight
W_{fuel}	Fuel Weight
$W_{fuselage}$	Body Weight
$W_{HStable}$	Horizontal Stabilizer Weight
W_{hub}	Main Rotor Hub Weight
$W_{instruments}$	Instruments Weight
W_{LG}	Landing Gear Weight
W_{pusher}	Pusher Propeller Weight
W_t	Tooth Loading Force (lbs)
$W_{VStable}$	Vertical Stabilizer Weight
x_{cg}	Center of Gravity From Main Rotor
Y	Rotor Side Force
α	Angle of Attack
β_{1c}	Longitudinal Flapping Angle
β_{1s}	Lateral Flapping Angle
β_o	Coning Angle
η	Auxiliary Propulsion Efficiency
θ_{1c}	Lateral Cyclic Pitch
θ_{1s}	Longitudinal Cyclic Pitch
θ_d	Differential Collective Pitch
θ_o	Collective Pitch
θ_{tw}	Blade Twist
κ	Rotor interference coefficient
λ	Rotor Inflow
μ_x, μ_z	Advance Ratios
ν_β	Natural Flapping Frequency
ρ	density
σ	Blade Solidity
φ	Bank Angle
χ	Skew Angle
Ω	Rotor Rotational Velocity
$\Omega 2$	Reduced Rotor Rotational Velocity
ΩR	Hover Tip Speed

Works Cited

Committee, A. B. (1974). *AGMA Standard Design Procedure for Aircraft Engine and Power Take-Off Bevel Gear .* Alexandria, Virginia: Reproduced by Global Engineering Documents with Permission of AGMA.

Hepperle, M. (2003, August 09). *JavaProp - Design and Analysis of Propellers*. Retrieved March 07, 2011, from Aerodynamics of Model Aircraft: http://www.mh-aerotools.de/airfoils/javaprop.htm

Leishman, G. (2006). *Principles of Helicopter Aerdynamics.* New York: Camridge University Press.

Prouty, R. W. (1995). *Helicopter Performance, Stability, and Control.* Malabar, Florida: Krieger Publishing Company, INC.

Shigley, J. E. (1996). *Standard Handbook of Machine Design 2nd Ed.* New York: McGraw-Hill Companies Inc.

Appendix

Totals	48	52	49	42	45	46	45	38
Rank	3	1	2	7	6	4	5	8
	Concept 1 Ducted Tilt Rotor	**Concept 2** Co-Axial Pusher Prop	**Concept 3** Small Tilt	**Concept 4** Co-Axial Jet	**Concept 5** Single Main Rotor Compound	**Concept 6** Oversized / NOTAR	**Concept 7** Compound Tandem	**Concept 8** Lifting Body
Performance								
Range	3	3	3	2	2	2	3	2
Speed	3	3	3	3	2	3	2	1
Payload	3	3	3	3	3	3	3	3
Agility	3	3	3	2	2	3	2	2
Hover Perform	2	3	2	2	3	3	3	1
Forward Flight	3	3	3	3	2	2	2	2
Attributes								
Weight	2	3	3	1	3	2	2	3
Interior Size	3	3	3	2	3	1	3	2
Noise	2	2	2	1	2	3	2	2
Complexity	2	2	2	2	2	2	2	1
Aerodynamics	2	2	3	2	2	3	2	3
Configurability	3	3	3	3	3	2	3	3
Affordability								
Flyaway Cost	2	2	2	2	2	2	2	1
Maintainability	3	3	3	3	3	2	3	2
Operating Cost	2	2	2	2	2	2	2	2
Feasibility								
TRL (COTS)	3	3	3	3	3	2	3	1
Other Qualities								
Innovation	3	4	2	2	2	5	2	3
Safety	2	3	2	2	2	2	2	2
Survivability	2	2	2	2	2	2	2	2

Performance Inputs:

W – 16,415 lb
f – 25 ft^2
x_{cg} – 4 in
h_{cg} – 5 ft
R – 22.5 ft
Ω – 30.2 rad/s (288.6 rpm)

Ω2 – 21.8 rad/s (208.4 rpm)
ν_β – 1.6
S_r – 3.3 ft
κ– 1.22
σ – 0.12
θ_{tw} – -10°

a – 6.857
M_{dd} – 0.78
η – $(-3e4*v^2+0.136v+64.8)/100$
C_{Do} – 0.008

Table 10: 6K95 ($\rho = 0.001781$ sl/ft^3) Performance Values

u (kts)	T_{rotor} (lb)	T_{aux} (lb)	P_{rotor} (hp)	P_{aux} (hp)	P_{tot} (hp)
0	16843	0	1628	0	1628
10	16843	0	1575	0	1575
20	16849	0	1433	0	1433
30	16867	0	1260	0	1260
40	16895	0	1114	0	1114
50	16950	0	1013	0	1013
60	16182	0	902	0	902
70	16295	0	877	0	877
80	16469	0	880	0	880
90	16721	0	906	0	906
100	17074	0	956	0	956
110	17567	0	1033	0	1033
120	16719	913	458	438	895
130	17059	1072	457	552	1009
140	17158	1243	467	685	1152
145	17299	1333	473	759	1232
150	17455	1427	481	837	1318
155	17628	1524	490	921	1412
160	17819	1624	502	1011	1512
170	18272	1833	531	1207	1738
180	18779	2055	568	1427	1995
190	19370	2289	615	1673	2288
200	20021	2537	671	1947	2618
210	20649	2797	731	2250	2981
220	21250	3069	792	2585	3377
230	21779	3355	851	2953	3804
240	22219	3653	904	3358	4261
250	22573	3964	951	3800	4847

Table 11: Sea level (ρ = 0.002378 sl/ft^3) Performance Values

u (kts)	T_{rotor} (lb)	T_{aux} (lb)	P_{rotor} (hp)	P_{aux} (hp)	P_{tot} (hp)
0	16843	0	1592	0	1592
10	16842	0	1530	0	1530
20	16851	0	1377	0	1377
30	16879	0	1210	0	1210
40	16919	0	1088	0	1088
50	16999	0	1015	0	1015
60	16280	0	946	0	946
70	16479	0	949	0	949
80	16781	0	980	0	980
90	17222	0	1039	0	1039
100	17861	0	1128	0	1128
110	18770	0	1255	0	1255
120	17056	1219	476	585	1061
130	17399	1431	490	737	1227
140	17815	1660	510	915	1425
145	18077	1780	525	1013	1537
150	18372	1905	541	1118	1659
155	18704	2034	561	1230	1791
160	19083	2168	585	1349	1935
170	19983	2447	646	1611	2257
180	21063	2744	726	1905	2631
190	22250	3057	824	2234	3058
200	23404	3387	929	2599	3528
210	24395	3734	1029	3004	4033
220	25160	4098	1112	3451	4563
230	25707	4479	1179	3943	5207
240	26078	4877	1230	4483	6009
250	26318	5292	1271	5074	6889